

Center Projection Vortices in Continuum Yang-Mills Theory

M. Engelhardt¹ and H. Reinhardt²

*Institut für Theoretische Physik, Universität Tübingen
D-72076 Tübingen, Germany*

Abstract

The maximal center gauge, combined with center projection, is a means to associate Yang-Mills lattice gauge configurations with closed center vortex world-surfaces. This technique allows to study center vortex physics in lattice gauge experiments. In the present work, the continuum analogue of the maximal center gauge is constructed. This sheds new light on the meaning of the procedure on the lattice and leads to a sketch of an effective vortex theory in the continuum. Furthermore, the manner in which center vortex configurations generate the Pontryagin index is investigated. The Pontryagin index is built up from self-intersections of the vortex world-surfaces, where it is crucial that the surfaces be globally non-oriented.

PACS: 11.15.-q, 12.38.Aw

Keywords: Yang-Mills theory, center vortices, maximal center gauge, Pontryagin index

¹Supported by DFG under grant number DFG En 415/1-1

²Supported in part by DFG under grant number DFG Re 856/4-1

1 Introduction

The infrared sector of strong interaction physics is characterized by nonperturbative phenomena such as confinement, the breaking of chiral symmetry, and the $U_A(1)$ problem. These phenomena are believed to be described by quantum chromodynamics; however, in order to understand in more detail how they arise, it is helpful to isolate the particular degrees of freedom of the theory which induce these phenomena. Chiral symmetry breaking and the $U_A(1)$ problem can e.g. be successfully explained in terms of instanton effects [1], whereas confinement eludes a description via instantons [2].

Viable explanations of confinement can be based on magnetic degrees of freedom such as Abelian magnetic monopoles [3] or center vortices [4],[5]; considerable evidence in favor of such scenarios has accumulated in recent years from numerical lattice studies. Magnetic monopoles emerge in Yang-Mills theory as gauge fixing defects in the so-called Abelian gauges [6], where the Cartan subgroup of the gauge group under consideration is left unfixed. In all Abelian gauges considered, the vacuum behaves as a dual superconductor [7]; in particular, lattice calculations performed in the maximal Abelian gauge [8],[9] exhibit Abelian and monopole dominance for the string tension. On the other hand, lattice calculations performed in the so-called maximal center gauge [10], which will be discussed in detail in this work, have provided evidence in favor of the notion that confinement is induced by center vortices. The vortex content of gauge field configurations produces virtually the full string tension; conversely, the string tension disappears in the absence of vortices [10]. This property of *center dominance* persists at finite temperatures [11],[12], and the deconfinement phase transition can be understood as a transition from a percolating vortex phase to a phase in which the vortices cease to percolate.

The aforementioned magnetic degrees of freedom inducing confinement can furthermore be connected with the topological properties commonly thought to be carried by instantons; they may therefore ultimately be suited to provide a unified picture of the different nonperturbative strong interaction phenomena mentioned further above. The magnetic monopoles of the maximal Abelian gauge have been empirically found to be correlated with instantons in lattice calculations [13]. In another Abelian gauge, the Polyakov gauge, the Pontryagin index can be entirely reconstructed from the magnetic monopole content of gauge field configurations [14]. On the other hand, one of the foci of the present work is to elucidate the manner in which center vortex

configurations generate the Pontryagin index; it will be shown that the latter is produced by self-intersections of vortex world-surfaces, where it is crucial that the surfaces be globally non-oriented. In a recent lattice study [15], the orientability of the vortex surfaces was studied, with the result that these surfaces are non-orientable in the confining phase and have non-trivial genus. Furthermore, in an ensemble devoid of vortices, chiral symmetry breaking disappears and all configurations belong to the trivial topological sector [16].

For the abovementioned lattice studies of vortex properties to become possible, techniques had to be developed which allow to associate a given lattice gauge configuration with a configuration of vortex world-surfaces. Such techniques have only become available in relatively recent times; this has revived interest in the vortex picture, which received rather little attention after some early efforts following its inception [4],[5],[17]. The techniques referred to here are the maximal center gauge and center projection [10],[18] already mentioned further above. While not all questions concerning the numerical stability of this procedure and its ability to faithfully represent thick center fluxes present in full gauge configurations have been settled [19], it has facilitated a number of observations concerning vortex physics in addition to those already mentioned further above. E.g., the density of the center vortices obtained via the maximal center gauge and center projection displays the proper scaling behavior required under the renormalization group and, consequently, these vortices can be considered as physical objects [20] (note erratum in [11]), see also [21]. Also binary correlations of vortex intersection points found on a given space-time plane display such scaling [22]. Furthermore, center vortices can account for the Casimir scaling behavior of the adjoint string tension if one associates a finite physical thickness with the vortex world-surfaces [23],[24]. In an indirect version of the maximal center gauge, which proceeds via an intermediate maximal Abelian gauge fixing, both Abelian magnetic monopoles and center vortices were detected [18]; the monopoles were found to be located on center vortices like beads on a string.

One of the foremost aims of this work is to develop a continuum formulation for the center gauge and center projection procedure. This will also shed some additional light on issues concerning the procedure on the lattice. It should be clear that the attempt to construct an analogue of the maximal center gauge in the continuum encounters some conceptual obstacles not found in continuum formulations of Abelian gauges, which are quite straightforward.

These obstacles are related to the fact that the continuum theory is constructed in terms of a gauge potential, defined in the adjoint representation of the gauge group, as opposed to the lattice formulation in terms of group elements on lattice links. The continuum gauge fields are thus insensitive to the center of the gauge group. It is a priori not clear how to extend the successful concept of center projection to the continuum theory. Nevertheless, it will prove possible in this work to derive a continuum analogue of the lattice procedure.

In detail, the plan of this paper is as follows. In section 2, the maximal center gauge and the emergence of center vortices after center projection is carefully analyzed on the lattice. The effect of this gauge on sample gauge fields of the vortex type is studied empirically; subsequently, the gauge fixing procedure on the lattice is reformulated in a manner which explicitly separates the $Z(N)$ center and $SU(N)/Z(N)$ coset degrees of freedom. The continuum limit of center and coset lattice configurations is considered in section 3, along with the gauge transformations which arise in the course of maximal center gauge fixing. Explicit continuum representations of center vortices are given. This allows the construction of the continuum analogue of the maximal center gauge, the properties of which are then discussed extensively, including alternative formulations which allow to extract more general objects of the vortex type; for reasons mentioned further above, vortex surfaces made up of patches of different orientation are of particular interest, as well as thickened vortices. In section 4, the implementation of the maximal center gauge in the continuum path integral is considered, and a sketch of an effective vortex theory is given. Finally, the Pontryagin index generated by center vortex configurations is studied in section 5. The concluding section 6 discusses some open issues to be settled in subsequent work. Some mathematical details are presented in the appendices.

2 Maximal Center Gauge and Center Vortices

2.1 The Maximal Center Gauge

Maximal center gauge is a gauge fixing condition defined in the lattice formulation of $SU(N)$ Yang-Mills theory. It prescribes that the gauge freedom

$$U_\mu(x) \rightarrow U_\mu^V(x) = V(x + e_\mu)U_\mu(x)V^\dagger(x) \quad (1)$$

be used to transform the link variables $U_\mu(x)$ of a given lattice configuration as close as possible to center elements of the gauge group, in a sense still to be specified. In fact, there exist many different specifications, or realizations, of the general idea formulated above. One possible explicit gauge fixing condition, first introduced in [18] for the case of $SU(2)$ color³ as the “Direct Maximal Center Gauge”, is

$$\max_V \sum_{x,\mu} \left| \text{tr} U_\mu^V(x) \right|^2 \quad (2)$$

for arbitrary local $SU(2)$ gauge transformations V .

In order to make this more transparent, represent the $SU(2)$ link variables as

$$U = c_0 + i\vec{c}\vec{\tau} \quad (3)$$

where τ_i denotes the Pauli matrices and the parameters $c_0, c_i, i = 1, 2, 3$, fulfil the constraint

$$c_0^2 + \vec{c}^2 = 1 \quad (4)$$

to guarantee unitarity of the links. Note that (4) defines a three-sphere in the space of parameters c_0, c_i . In the following, the set of group elements with $c_0 > 0$ will sometimes be referred to as the “northern hemisphere” of the $SU(2)$ group, and the set of group elements with $c_0 < 0$ as the “southern hemisphere”. The poles of the sphere, $c_0 = \pm 1$, correspond to the center $Z(2)$ of the $SU(2)$ group. Correspondingly, the gauge condition (2) reduces to

$$\max_V \sum_{x,\mu} \left(c_{0,\mu}^V(x) \right)^2 \quad (5)$$

³Generalizations and applications to $SU(3)$ color were discussed in [21],[25].

which can be straightforwardly visualized in terms of a bias of the link variables towards the poles of the $SU(2)$ three-sphere.

An important property of the condition (2) is the fact that it leaves the center part of the gauge freedom, i.e. (for the general case of a $SU(N)$ gauge group) the $Z(N)$ part, unfixed. There is no bias distinguishing between different center elements due to the absolute value prescription in (2). This is analogous to the so-called Abelian gauges [6], which leave the Abelian part of the gauge freedom, i.e. the $[U(1)]^{N-1}$ part, unfixed.

The specific condition (2) is only one of many ways to bias link variables towards the center of the gauge group. In fact, any condition of the type

$$\max_V \sum_{x,\mu} \bar{g} \left(\left| \text{tr} U_\mu^V(x) \right| \right) \quad (6)$$

with a monotonously rising function \bar{g} implements the general idea of maximal center gauge fixing.

After transforming a lattice gauge configuration to the maximal center gauge, one can carry out a second step, called *center projection*, which serves to define the $Z(N)$ vortex content of the configuration. Center projection corresponds to mapping every link variable U onto the center element closest to U . In the case of the $SU(2)$ gauge group, this simply means mapping

$$U \rightarrow \text{sign tr } U , \quad (7)$$

i.e.

$$c_0 \rightarrow \text{sign } c_0 . \quad (8)$$

In other words, all link variables located on the northern hemisphere are mapped onto the north pole of the $SU(2)$ group, all links on the southern hemisphere onto the south pole. For general $SU(N)$ group, center projection leaves one with a $Z(N)$ lattice, which in the canonical fashion can be associated with $(D - 2)$ -dimensional vortex surfaces (where D denotes the space-time dimension) on the dual lattice: If any plaquette on the $Z(N)$ lattice evaluates to a nontrivial center element, it is considered to be pierced by a vortex carrying the appropriate (quantized) flux; if it takes the trivial value unity, no vortex pierces the plaquette. The vortices defined in this way represent $(D - 2)$ -dimensional surfaces in D space-time dimensions. The center flux carried by the vortices is continuous; there are no sources or sinks for this flux. In the case of a $Z(2)$ lattice, this corresponds to the vortex surfaces being closed. In the general $Z(N)$ case, the surfaces may branch,

while respecting flux conservation, since more than one nontrivial center flux exists. However, precisely due to flux conservation, one may think also of such branched surfaces in the $Z(N)$ case as being composed of simple closed surfaces which in general share whole surface patches in space-time.

2.2 Center vortices on the lattice

For the purpose of illustrating the effect of the center gauge condition, consider the following sample continuum $SU(2)$ gauge field configurations on a two-dimensional plane. Let the plane be parametrized in polar coordinates r, φ and define the gauge field as⁴

$$a_\varphi = \pm \frac{1}{r} T_3, \quad a_r = 0 \quad (9)$$

This configuration, and the ones to follow below, can be regarded as slices of configurations defined in more space-time dimensions, and which, for the present purposes, can be considered constant in the additional dimensions. Also the Lorentz components of the gauge field associated with those additional directions should be considered to vanish. The above configuration is a particular example of what in the following will be called a *thin vortex* (positioned at the origin of the plane). A general representation of thin vortices will be given in eq. (62). The defining property of a thin vortex is that any Wilson loop which encircles the vortex, i.e. in the present case, the origin, takes a nontrivial value in the center of the gauge group. For the case of $SU(2)$ color, this corresponds to the value (-1) . On the other hand, any other Wilson loop, not encircling the vortex, takes the value $(+1)$. In other words, the vortex contributes a nontrivial center element of the gauge group to any Wilson loop it pierces. Correspondingly, the field strength is singular and localized at the position of the vortex. Note that both choices of sign in (9) lead to these properties. Thus, one can distinguish two different orientations of vortices, associated with the direction of (magnetic) flux they describe (flux which is dual to Wilson loops will sometimes be referred to as “magnetic” in the following). On the other hand, also (odd) integral multiples of the configurations (9) satisfy the defining properties of

⁴Gauge fields in the following are decomposed using antisymmetric generators T_a of the gauge group satisfying $[T_a, T_b] = f_{abc} T_c$, with f_{abc} denoting the structure coefficients, and the normalization $\text{Tr} T_a T_b = -\delta_{ab}/2$. For $SU(2)$, $T_a = -i\tau_a/2$, where τ_a , $a = 1, 2, 3$, denotes the Pauli matrices.

center vortices. However, such configurations will not be considered as distinct types of vortices, but simply as superpositions of vortices of the smallest Abelian magnetic flux required to induce the center element in question in a Wilson loop.

Consider furthermore the more general configuration

$$A_\varphi = \pm \frac{f(r)}{r} T_3, \quad A_r = 0 \quad (10)$$

with $f(0) = 0$ and $f(\infty) = 1$. This configuration represents a *thick vortex*; in order for a Wilson loop to take the value (-1) , it must circumscribe the vortex at a sufficient distance, the thickness of the vortex, determined by the form of the *profile function* $f(r)$. Also the field strength or the flux associated with a thick vortex are spread out as compared to the singular localized field strength of a thin vortex (9). For certain purposes, such as calculating field strengths, it may be necessary to specify more precisely what one means by the singularity of the thin vortex (9) at the origin; this becomes relevant e.g. in Appendix C. In such a case, the thin vortex should always be viewed as the limit in which $f(r) \rightarrow 1$ for $r \neq 0$, but still $f(r = 0) = 0$ in (10).

These configurations can be put on a two-dimensional lattice in the canonical fashion by associating the path-ordered exponential

$$U_\mu(x) = \mathcal{P} \exp \left(- \int_P A_\mu(z) dz_\mu \right) \quad (11)$$

with a link $U_\mu(x)$ describing a path P originating from the point x and running in the μ -direction. Note that path-ordering \mathcal{P} is not actually necessary for the Abelian configurations (9) and (10). This procedure of putting the continuum configurations on the lattice preserves the values of Wilson loops taken in the corresponding configurations, as described above.

In practice, it is desirable to treat a lattice of finite extent with periodic boundary conditions, i.e. a lattice torus. In order to fulfil such boundary conditions, it is necessary to have zero net flux piercing the plane under consideration⁵. For this reason, in the following, linear superpositions of pairs of (thin or thick) vortices of opposite orientation will be examined,

⁵Consider a Wilson loop running around the edge of the lattice. Due to the periodic boundary conditions and the Abelian character of the configurations treated here, contributions from opposite sides of the loop cancel and the Wilson loop must take the value $(+1)$.

cf. Fig. 1 (a). Due to the Abelian character of the configurations defined above, the phases contributed to Wilson loops by single vortices in a many-vortex superposition simply add, without interference from path-ordering effects. Furthermore, in calculating the lattice links from the gauge fields, also the contributions from periodic images of the vortices must be taken into account⁶.

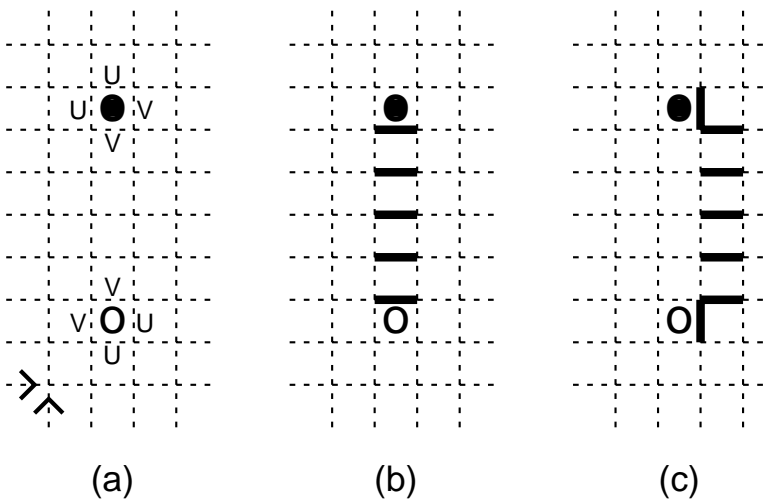


Figure 1: Two thin SU(2) vortices, cf. eq. (9), placed on a space-time lattice (a), where the arrows in the lower left-hand corner specify the direction of the line integrals defining horizontal and vertical links, respectively. The open and filled circles denote the locations of the vortices, the difference in the symbols signifying that the vortices have opposite orientation. In (a), all lattice links deviate from unity, but all plaquettes multiply to (+1), except the plaquettes pierced by vortices, which multiply to (-1). The links making up those latter plaquettes take the values $U = \exp(T_3\pi/2)$ and $V = U^\dagger$ (up to small corrections from the respectively other vortex). After maximal center gauge fixing (b), all lattice links take the value (+1), except the ones displayed in fat print, which take the value (-1). There are alternative gauge fixing images, such as (c), for which the center gauge fixing functional is degenerate, and which are related to the configuration (b) by gauge transformations purely from the center of the gauge group.

⁶In practice, for better convergence of this sum, the authors covered the plane with positively and negatively oriented vortices in checkerboard fashion. Therefore, the lattice torus actually used in numerical computation contained four vortices as opposed to the two displayed in Fig. 1. This is merely a point of technical convenience.

Having put the gauge configurations on the lattice, the question can be addressed what effect the center gauge fixing procedure has on these configurations. For the case of two thin vortices, fixing the configuration depicted in Fig. 1 (a) to maximal center gauge can be carried out trivially without any recourse to numerical computation. All one needs are the following two observations: The configuration shown in Fig. 1 (b) is gauge equivalent to the one shown in Fig. 1 (a) since all Wilson loops take the same values in the two configurations. At the same time, in Fig. 1 (b) all links take values in the center of the gauge group. Therefore, this configuration realizes the maximal possible value of the gauge fixing functional (6). Thus, the configuration shown in Fig. 1 (b) is precisely a center gauge fixing image of the configuration shown in Fig. 1 (a). It is described by a string of links taking a value corresponding to a nontrivial center element extending from the position of one thin vortex to the position of the other. This type of configuration, i.e. strings of links associated with a nontrivial center element of the gauge group, will in the following be termed a configuration of *ideal vortices*. It is, as just seen, gauge equivalent to a configuration of *thin vortices* at the positions where the strings end.

It should be noted that there exist many other degenerate maxima of the gauge fixing functional on the same gauge orbit, namely all deformations of the string of links, cf. Fig. 1 (c). These are all images of the configuration shown in Fig. 1 (b) under gauge transformations which are elements of the center of the gauge group. This is not surprising; by construction, the gauge fixing condition (6) is invariant under such transformations (e.g. in the $SU(2)$ case, it is insensitive to the sign of the link variables). In other words, it leaves the center of the gauge group unfixed. As a consequence, the precise trajectory of the string of nontrivial links describing ideal vortices is arbitrary; only its two endpoints (corresponding here to the positions of the two thin vortices) are fixed, and they embody all gauge-invariant information.

Note that in three-dimensional space-time, the sets of nontrivial links describing ideal vortices generically form two-dimensional sheets, whereas in four-dimensional space-time, they form three-dimensional volumes. The boundaries of the sheets or volumes, respectively, describe the locations of the thin vortices to which the ideal vortex configuration is gauge equivalent.

As a further aside, note that center projection leaves the center gauge fixed configuration (Fig. 1 (b)) unchanged and thus does not truncate any physical information contained in it. By contrast, center projecting the original

configuration (Fig. 1 (a)) before gauge fixing completely removes the vortices and yields a trivial lattice with all links at unity.

Continuing to the case of a thick vortex, it is clear that this case cannot be solved in a similarly trivial fashion. Here, the latticized gauge configurations can be brought into the maximal center gauge numerically by maximizing the gauge functional (6) under the action of arbitrary $SU(2)$ gauge transformations on the sites of the lattice. As described above, lattice tori containing four vortices were used. Two different cases were examined: Two thick vortices of one orientation together with two thin vortices of the other orientation (cf. Fig. 2 (a)), and one thick vortex together with three thin vortices, again such that the total flux piercing the plane vanishes (cf. Fig. 2 (b)). In order to make the new effects arising in the case of a thick vortex more visible, a Fermi distribution

$$f(r) = 1 - \frac{1}{1 + \exp(5(r - 4l)/l)} \quad (12)$$

where l denotes the lattice spacing, was chosen for the profile function $f(r)$ (cf. eq. (10)). This not only spreads out the flux of the vortex but actually localizes it on a ring of radius $4l$ concentric to the core of the vortex.

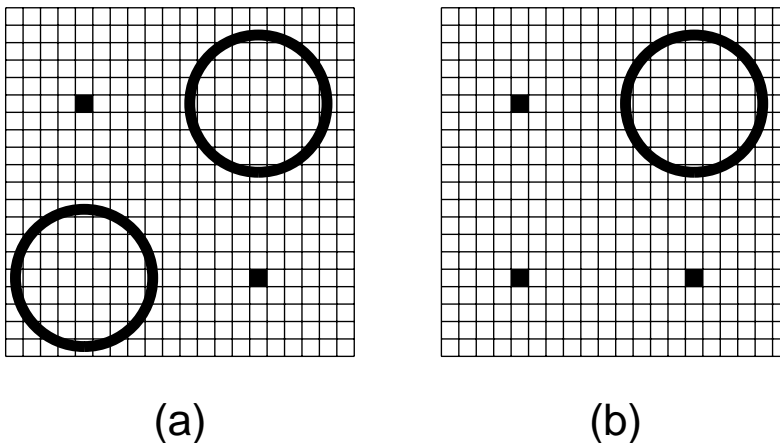


Figure 2: Configurations containing thin vortices and thick vortices, the flux of the latter being concentrated on the displayed rings. These configurations can be transformed into the maximal center gauge numerically (see text).

The gauge equivalent configurations which maximize the center gauge fixing functional (6) will contain a certain set of links which lie in the “southern hemisphere” of the $SU(2)$ group, i.e. nearer to the center element (-1) , whereas the other links remain closer to the center element $(+1)$. Center projection then associates a collection of ideal vortices, or, gauge-equivalently, thin vortices, with the original configuration. Carrying out this procedure numerically for the configurations depicted in Fig. 2, one obtains thin vortices which approximate the locations of the original thick vortices; however, the precise location of the thin vortex within the profile of the thick vortex turns out to depend on the precise realization of the center gauge via the arbitrary function \bar{g} in the gauge fixing functional (6). Specifically, for the configuration containing one thick vortex, Fig. 2 (b), it turns out that for the gauge fixing function $\bar{g}(t) = t^2$, the thin vortex is located concentrically with the thick vortex, whereas for $\bar{g}(t) = 1 - \theta(2 - t)(1 - t^2/4)^2$, the thin vortex is located one lattice spacing away from the center of the thick vortex. This latter effect becomes more pronounced if one uses the configuration with two thick vortices, Fig. 2 (a), again with the gauge fixing function $\bar{g}(t) = 1 - \theta(2 - t)(1 - t^2/4)^2$. There, the thin vortex is located four lattice spacings away from the center of the thick vortex, i.e. on the ring of flux depicted in Fig. 2 (a).

The conclusion reached from these examples is therefore that the maximal center gauge does yield thin vortices which roughly approximate the locations of thick vortices in gauge field configurations. This corroborates the findings of [10],[25]; note however recent indications of considerable instability in the numerical gauge-fixing procedure [19]. Furthermore, the precise coordinates of the thin center projection vortices turn out to be gauge-dependent, via the gauge fixing function \bar{g} . Also, comparing the results obtained with the two different configurations depicted in Fig. 2, the precise location of a thin vortex approximating a given thick vortex evidently also depends on the structure of other vortices in the vicinity. Therefore, it seems that the center gauge fixing procedure introduces nonlocal interactions into the center projection vortex effective theory independent of any reference to the Yang-Mills dynamics which ultimately governs the original thick vortex configurations.

2.3 Separating center and coset degrees of freedom

In the attempt to formulate an analogue of the center gauge and center projection procedure in continuum Yang-Mills theory, one obviously encounters

a conceptual obstacle: Continuum Yang-Mills theory is described in terms of a gauge potential $A_\mu^a(x)$ which is defined in the adjoint representation of the gauge group. Thus, in the continuum, the gauge symmetry of Yang-Mills theory is only a local $SU(N)/Z(N)$, i.e. a coset, symmetry. Related considerations concerning this issue in the Schrödinger picture can be found in [26]. The first step in dealing with this problem is to carefully separate center and coset degrees of freedom in the lattice gauge fixing procedure discussed above. The treatment below will for simplicity mainly concentrate on the case of an $SU(2)$ gauge group; however, the generalization to any $SU(N)$ group is conceptually, if not necessarily notationally, straightforward. One only has to keep in mind that higher $SU(N)$ groups have more center elements, and that therefore there are more species of vortices, corresponding to the different possible fluxes. The only qualitative difference in terms of the topology of vortex configurations is that, for higher gauge groups (and three or more space-time dimensions), vortices may branch into several vortices with different center fluxes, as long as flux conservation is respected at branchings.

To have a slightly more precise terminology at hand in the discussion below, it is useful to decompose the link variables $U_\mu(x)$ describing a $SU(2)$ lattice configuration into a center part

$$Z_\mu(x) = \text{sign tr } U_\mu(x) \tag{13}$$

and a coset part $U'_\mu(x)$ defined by

$$U_\mu(x) = Z_\mu(x)U'_\mu(x) . \tag{14}$$

The lattice described by $Z_\mu(x)$ will be referred to as the *center part* of the lattice configuration $U_\mu(x)$, whereas the lattice described by $U'_\mu(x)$ will be referred to as the *coset part*. Note that the center gauge fixing functional (6) depends only on the coset part of a configuration; center projection simply means mapping $U_\mu(x)$ onto $Z_\mu(x)$.

Furthermore, below the terminology *coset transformation* will be used to characterize gauge transformations, cf. eq. (1), which change only the coset part of a lattice configuration. Note that this does not imply that the corresponding unitary transformation matrices acting at lattice sites are necessarily from the northern hemisphere of the $SU(2)$ group. Note furthermore that the set of possible coset transformations depends on the initial gauge

configuration and that in general not all members of this set can be continuously deformed to the identity while remaining in the set. Also, smooth gauge transformations G in the continuum formulation of Yang-Mills theory,

$$A_\mu \longrightarrow A_\mu^G = G(A_\mu + \partial_\mu)G^\dagger \quad (15)$$

are by construction coset gauge transformations.

Clearly, if one puts a smooth continuum gauge configuration $A_\mu(x)$ onto a sufficiently fine lattice, the associated center part is trivial, $Z_\mu(x) = 1$. However, even in such a case, gauge fixing in general, and the center gauge fixing procedure in particular, may induce a nontrivial center part in the gauge fixed lattice; explicit examples were given in the previous section. In other words, some links in the gauge fixed lattice end up in the southern hemisphere, i.e. closer to the nontrivial center element (-1) than to the trivial element $(+1)$; ideal vortices are introduced.

In the $SU(2)$ lattice description of the center gauge fixing procedure, one allows arbitrary $SU(2)$ gauge transformations when maximizing the gauge fixing functional (6). This procedure can be broken down into smaller steps as follows.

1. Start from a configuration with a trivial center part, i.e. with all links in the northern hemisphere, such as one obtains by putting any smooth continuum gauge configuration onto a sufficiently fine lattice. Apply a gauge transformation which rotates a certain arbitrary, but fixed, set of links to the southern hemisphere, i.e. such that the center part of the transformed lattice displays the nontrivial value (-1) on that set of links⁷.
2. Maximize the gauge fixing functional using only coset transformations, i.e. keeping the center part of the configuration invariant. In other words, links are not allowed to switch “hemispheres” of the $SU(2)$ group. Note that this second step operates purely on the coset part of the lattice configuration obtained after step 1.) above; not only are

⁷As long as the original links are sufficiently close to unity (which one can always achieve by choosing the lattice spacing accordingly), this transformation can e.g. be effected by applying the group element $V = \exp(2\pi T_3/3)$ to the site from which the links in question emanate and the group element V^\dagger to the site at which they end, i.e. $U \rightarrow VUV$, where U denotes the original link variable associated with the link under consideration. One can also exchange V and V^\dagger , which may become necessary if two links in question share a site.

only coset transformations allowed, but also the gauge fixing functional (6) depends exclusively on the coset part of the link variables.

3. Finally, this two step procedure must be repeated for all possible first step choices of the center part of the transformed lattice, in order to cover all possible gauge transformations contained in the full $SU(2)$ gauge group. For each of these choices, corresponding to a certain ideal vortex configuration, one obtains in the associated second step a constrained maximum of the gauge fixing functional (6); from all these maxima, one must choose the highest one in order to obtain the gauge-fixed configuration reached under the action of the full $SU(2)$ gauge group.

Slightly rephrased, the procedure described above splits the process of center gauge fixing under the $SU(2)$ gauge group up into the following parts: One introduces, by a suitable gauge transformation, into an initially smooth gauge configuration ideal vortices at fixed, but arbitrary, locations. This step transfers information from the coset part into the center part of the configuration. From this point onwards, however, center and coset parts remain strictly separated and subsequent gauge transformations operate only on the coset part. The latter is transformed, by using purely coset transformations, to the (constrained) maximum of the (purely coset-dependent) gauge fixing functional (6). The algorithm must be repeated for all possible choices of ideal vortex configurations. The choice which leads to the global maximum of the gauge fixing functional determines the center gauge and center projection image of the original configuration.

Formally, one can summarize this as follows. The center gauge fixing condition, cf. eq. (6), corresponds to the two-fold maximization problem

$$\max_Z \max_G \sum_{x,\mu} \bar{g} \left(\left| \text{tr} \left((U_\mu(x)^{V[Z]})'^G \right) \right| \right) \quad (16)$$

where $U_\mu(x)$ is the gauge configuration one starts with and Z denotes the center part of the transformed lattice chosen in step 1.) above, realized by the gauge transformation $V[Z]$ as specified there. The prime emphasizes explicitly that only the coset part of the resulting configuration is considered further, although this is already guaranteed by the absolute value prescription. In other words, the configurations $(U^V)'$ are stripped of all ideal vortices. Finally, G denotes all coset gauge transformations considered in step 2.) above.

3 Taking the continuum limit

3.1 Continuum limit of lattice configurations

As the first step in formulating a continuum version of the maximal center gauge, it is necessary to define the continuum analogues of the various lattice configurations considered above.

3.1.1 Continuum limit of the coset part

The coset part of a lattice configuration can be directly associated with a regular continuum gauge field constructed such as to reproduce all links of the coset configuration if put on the lattice. One could e.g. achieve this construction by giving an “inverse blocking” prescription, successively replacing coarser by finer lattices while dividing up the phases carried by the coarse links onto the fine links such as to achieve a smooth continuum limit. In this limit, it will be possible to expand an exponential representation of the link variables

$$U'_\mu(x) = \exp(-lA'_\mu(x)) \tag{17}$$

into powers of the lattice spacing l and regard $A'_\mu(x)$ as the continuum gauge field. As a side remark, note that if one wished to apply such an “inverse blocking” procedure to the center part of a configuration, the corresponding prescription would have to be radically different in order to preserve the center, or ideal vortex, character of the configuration: If a nontrivial center link of a coarse lattice is divided up into two links of a finer lattice, the whole nontrivial center phase would have to be associated with one of the two links, whereas the other link would be associated with unity. The phase is not divided up among the two links, in contrast to the coset case, and the continuum limit is singular. In particular, expanding an exponential representation analogous to (17) is by construction never possible for the center part of a configuration. Due to these difficulties, a different approach will have to be taken when discussing the continuum limit of the center part below.

Before proceeding, it is worth noting that the gauge freedom associated with the continuum gauge field A'_μ in (17) matches the one associated with the coset lattice U'_μ in step 2.) of the center gauge fixing procedure as described in section 2.3; namely, it consists of all possible coset transformations. Thus, in describing a coset lattice in the continuum limit by means of a gauge

field A'_μ as in (17), one is not introducing any restriction on the residual gauge freedom allowed in step 2.) of the center gauge fixing procedure. The additional gauge freedom implied by the full $SU(N)$ symmetry present in lattice Yang-Mills theory has been explicitly separated off into the choice of ideal vortex configuration in step 1.).

3.1.2 Continuum limit of the center part

The center part of a configuration contains exclusively ideal vortices, described by sets of links taking a nontrivial value from the center of the gauge group. At this point, it is useful to give an alternative characterization of such a configuration which does not make explicit reference to a space-time lattice. This can be achieved via the effect the configuration has on arbitrary Wilson lines. Consider therefore calculating an arbitrary Wilson line; as one travels along the line, gathering up phases from the different links making up the path, the Wilson line either stays constant or picks up a phase corresponding to a nontrivial element from the center of the gauge group on a length of one lattice spacing l . Expressed through the vortex content, this latter change happens whenever the Wilson line intersects a string, surface, or volume of nontrivial links (depending on the space-time dimension) describing an ideal vortex configuration. As the lattice spacing is taken to zero, these strings, surfaces, or volumes become infinitely thin. Therefore, the continuum analogue of an ideal vortex configuration consists in specifying strings, surfaces, or volumes Σ (depending on the space-time dimension) which, when intersected by a Wilson line, contribute a center element factor to the latter.

3.2 Singular gauge transformations

In the previous sections, the effect of the maximal center gauge on vortex gauge fields originally defined in the continuum theory was investigated by first putting the Yang-Mills field on the lattice, subsequently implementing the maximal center gauge condition (which, so far, is defined only on the lattice) and afterwards considering again the continuum limit. One would, however, prefer not to use the detour via the lattice, but rather perform the maximal center gauge fixing directly in the continuum. Particular care is needed in defining the analogue of step 1.) of the maximal center gauge fixing procedure as laid out in section 2.3. It should be clear from the previous

discussion that this step in the continuum will introduce singularities (the ideal vortices) into the initially smooth gauge configurations. As already partly indicated above, these singularities are to be defined via their lattice origin, taking care in particular that gauge invariant quantities are unaffected by gauge transformations, even when the latter have a singular continuum limit. Keeping this methodology in mind, it will be possible to paraphrase the center gauge fixing procedure, as described step by step in section 2.3, directly in the continuum.

Consider a continuum Abelian gauge transformation $V(k, \Sigma, x)$ specified as follows. Let V be continuous everywhere except at hypersurfaces Σ of dimension $D - 1$ if D is the dimension of space-time. At such hypersurfaces, V shall have the following property. Let t denote the local coordinate perpendicular to Σ , with $t = 0$ on Σ , and let x_\perp denote the other local space-time coordinates. Then

$$\begin{aligned} V(k, \Sigma, x_\perp, t = \epsilon)V^\dagger(k, \Sigma, x_\perp, t = -\epsilon) &= Z(k) \\ V(\Sigma, x_\perp, t = -\epsilon)\partial_\mu V^\dagger(\Sigma, x_\perp, t = -\epsilon) &= V(\Sigma, x_\perp, t = \epsilon)\partial_\mu V^\dagger(\Sigma, x_\perp, t = \epsilon) \end{aligned} \quad (18)$$

where $\epsilon \rightarrow 0$ and k labels the $N - 1$ different nontrivial center elements $Z(k)$ of the $SU(N)$ gauge group under consideration. In other words, V jumps by a center phase $Z(k)$ at hypersurfaces Σ . An explicit realization of such a gauge transformation V will be given in the next section.

Consider applying a gauge transformation such as characterized above to an initial smooth field configuration A ,

$$A \rightarrow A^V = VAV^\dagger + V\partial V^\dagger \quad (19)$$

The first term on the right hand side still represents a smooth field everywhere except possibly on the edge $\partial\Sigma$ of Σ , since it is quadratic in V and hence insensitive to the center phase V picks up at hypersurfaces Σ . More care must be taken in properly defining the singularity in the second term. For this purpose, consider a Wilson line describing a straight-line path C from $(x_\perp, t = -\epsilon)$ to $(x_\perp, t = \epsilon)$, with x_\perp and t defined as above, and infinitesimal ϵ . Since the Wilson line transforms as

$$W[A](C) \rightarrow W[A^V](C) = V(x_\perp, t = \epsilon)W[A](C)V^\dagger(x_\perp, t = -\epsilon) \quad (20)$$

and furthermore $W[A](C) = 1 + O(\epsilon)$, one has

$$W[A^V](C) = Z(k) + O(\epsilon) \quad (21)$$

Therefore, the singularities of A^V at the hypersurfaces Σ describe nothing but an ideal vortex configuration $\mathcal{A}(\Sigma)$. On the other hand, the term $V\partial V^\dagger$ is a pure gauge. Therefore, the regular part of $V\partial V^\dagger$ must compensate the ideal vortex part described by the singularities at Σ such as to render all (closed) Wilson loops taken in the configuration $V\partial V^\dagger$ trivial. This means that $V\partial V^\dagger$ can be decomposed as⁸

$$V(\Sigma)\partial V^\dagger(\Sigma) = \mathcal{A}(\Sigma) - a(\partial\Sigma) \quad (22)$$

with the ideal vortex configuration $\mathcal{A}(\Sigma)$ localized on a hypersurface Σ , and a describing *thin vortices* localized on $\partial\Sigma$. The thin vortex field a can be defined on Σ as

$$\begin{aligned} a|_\Sigma &= -\lim_{\epsilon \rightarrow 0} V(\Sigma, x_\perp, t = -\epsilon)\partial V^\dagger(\Sigma, x_\perp, t = -\epsilon) \\ &= -\lim_{\epsilon \rightarrow 0} V(\Sigma, x_\perp, t = \epsilon)\partial V^\dagger(\Sigma, x_\perp, t = \epsilon) , \end{aligned} \quad (23)$$

cf. eqs. (18). Away from Σ ,

$$a = -V\partial V^\dagger \quad (24)$$

since the ideal vortex configuration $\mathcal{A}(\Sigma)$ only has support on Σ .

Before applying these singular gauge transformations to implement the maximal center gauge in continuum Yang-Mills theory, a few further properties should be noted for convenience. Given a general thin vortex configuration a , a corresponding gauge transformation V generating it can always be recovered via

$$V(y) = \exp\left(\int_{P(y_0, y)} a_\mu dx_\mu\right) \quad (25)$$

using an arbitrary fixed starting point y_0 . Path ordering is unnecessary, since a was constructed to be an Abelian field. Besides the trivial ambiguity in the choice of y_0 , which merely leaves a constant phase undetermined in V , there is a more important ambiguity, namely how the path $P(y_0, y)$ circumvents the locations of the thin vortices contained in a . This choice precisely determines the hypersurfaces Σ at which V jumps and which therefore describe the associated ideal vortex configuration \mathcal{A} .

From this, it also becomes clear that the thin vortex configuration a can be chosen independently of the precise singular surfaces Σ describing the

⁸The minus sign in front of $a(\partial\Sigma)$ is a convention introduced for later notational transparency.

associated ideal vortex configuration. Merely the boundary $\partial\Sigma$ must coincide with the location of the thin vortices contained in a . Indeed, given a transformation $V_1(\Sigma_1)$ inducing a thin vortex field a , one can explicitly give another transformation $V_2(\Sigma_2)$, with $\partial\Sigma_1 = \partial\Sigma_2$, generating the same field a as follows. Let M denote the interior of the closed hypersurface⁹ $\Sigma_1 \cup -\Sigma_2$. In D space-time dimensions, M is D -dimensional. Then define

$$V_2(k, \Sigma_2) = \begin{cases} Z(k)V_1(k, \Sigma_1) & \text{on } M \\ V_1(k, \Sigma_1) & \text{outside } M \end{cases} \quad (26)$$

This transformation generates the same thin vortex field a as $V_1(\Sigma_1)$ and an ideal vortex configuration described by the hypersurface Σ_2 . In particular, using $V_1(\Sigma_1)$ and $V_2(\Sigma_2)$, one can deform the ideal vortex part of an arbitrary gauge configuration without changing the configuration in any other respect:

$$(A + \mathcal{A}(\Sigma_1))^{V_1^{-1}V_2} = A + \mathcal{A}(\Sigma_2) \quad (27)$$

This is the continuum analogue of a transformation from the center of the gauge group. It exclusively deforms ideal vortices. Furthermore, the form of (26) shows that a homogeneous rotation of any gauge field is independent of the location of the singular hypersurfaces Σ ,

$$V_1(\Sigma_1)AV_1^\dagger(\Sigma_1) = V_2(\Sigma_2)AV_2^\dagger(\Sigma_2) \quad (28)$$

as long as V_1 and V_2 generate the same thin vortex field a , i.e. in particular $\partial\Sigma_1 = \partial\Sigma_2$.

As a simple example, consider the $SU(2)$ transformation

$$V = \exp(\varphi T_3) \quad (29)$$

in the plane described by the polar coordinates r, φ with $\varphi \in [0, 2\pi[$. At $\varphi = 0$, one has

$$V(r, \varphi = \epsilon)V^\dagger(r, \varphi = 2\pi - \epsilon) = -1 + O(\epsilon) \quad (30)$$

and, away from $\varphi = 0$,

$$a_\varphi = -\frac{1}{r}V\partial_\varphi V^\dagger = \frac{1}{r}T_3 \quad (31)$$

$$a_r = -V\partial_r V^\dagger = 0 \quad (32)$$

⁹The notation “ $-\Sigma$ ” is introduced to specify the orientation of a hypersurface. The hypersurface $-\Sigma$ is located on the same set of space-time points as the hypersurface Σ , but is associated with the reverse orientation.

i.e. one observes an ideal vortex at $\varphi = 0$ and a thin vortex (cf. eq. (9)) at the origin, $r = 0$. By simply changing the interval on which φ is defined (in general, as a function of r), one can arbitrarily deform the ideal vortex $\mathcal{A}(\Sigma)$ without changing $a(\partial\Sigma)$.

3.3 Continuum representation of center vortices

In the continuum limit, ideal vortex configurations $\mathcal{A}_\mu(k, \Sigma, x)$ are specified by hypersurfaces Σ (strings, sheets, or volumes in $D = 2, 3$ and 4 , respectively) which, when intersected by a Wilson line C , contribute a center element $Z(k)$ to the latter.

An explicit (singular) gauge field representation of an ideal vortex configuration in D space-time dimensions is given by

$$\mathcal{A}_\mu(x, \Sigma) = E \int_{\Sigma} d^{D-1} \tilde{\sigma}_\mu \delta^D(x - \bar{x}(\sigma)). \quad (33)$$

Here, Σ describes the infinitely thin continuum limit of the string, surface, or volume of nontrivial center element links making up the ideal vortex configuration. Σ is $D - 1$ -dimensional and its boundary $S = \partial\Sigma$ gives the location of the thin vortex $a_\mu(\partial\Sigma, x)$ to which the ideal vortex configuration $\mathcal{A}_\mu(\Sigma, x)$ is gauge equivalent (see below). Furthermore, $\bar{x}_\mu(\sigma) \equiv \bar{x}_\mu(\sigma_1, \sigma_2, \dots, \sigma_{D-1})$ denotes a parametrization of the $(D - 1)$ -dimensional hypersurface Σ . Also,

$$d^{D-1} \tilde{\sigma}_\mu = \frac{1}{(D-1)!} \epsilon_{\mu\alpha_1 \dots \alpha_{D-1}} d^{D-1} \sigma_{\alpha_1 \dots \alpha_{D-1}} \quad (34)$$

is the dual of the $(D - 1)$ -dimensional volume element

$$d^{D-1} \sigma_{\alpha_1 \dots \alpha_{D-1}} = \epsilon_{k_1 \dots k_{D-1}} \frac{\partial \bar{x}_{\alpha_1}}{\partial \sigma_{k_1}} \dots \frac{\partial \bar{x}_{\alpha_{D-1}}}{\partial \sigma_{k_{D-1}}} d\sigma_1 \dots d\sigma_{D-1}. \quad (35)$$

Note that these volume elements also define an orientation of the vortex. Like in the special case (9), in general two different orientations of vortices can be distinguished.

On the other hand, the color structure of the vortex is encoded in E . Note that the following discussion of the color factors E applies equally to thin vortices, to be treated in detail further below. The different kinds of vortex configurations introduced in this work are distinguished from one another only by their space-time structure, but they carry identical color structure.

It should furthermore be emphasized that the orientation of vortex flux is encoded already in the space-time structure, as mentioned above; this entails consequences regarding the set of color factors E necessary to generate all possible distinct vortex fluxes. For example, the substitution of E by $-E$ should not be considered to lead to a new class of vortices; the configurations generated by this substitution are already accounted for by keeping the original color structure E , but reversing the orientation of the hypersurface Σ in (33). As specified below, E should be restricted to a certain fundamental domain.

For the gauge group $SU(N)$, ideal center vortices in the continuum are given by eq. (33) with $E(k) = E_c(k)T_c$ satisfying

$$e^{-E(k)} = Z(k) , \quad k = 1, \dots, N-1 \quad (36)$$

where only generators T_c from the Cartan subalgebra are associated with non-vanishing coefficients $E_c(k)$, and $Z(k)$ denotes the $N-1$ nontrivial center elements of the $SU(N)$ group. The $E_c(k)$ can be considered as the components of vectors $E(k)$ in the Cartan subalgebra which, up to a factor 2π , coincide with the so-called co-weights $\mu(k)$, i.e. $E(k) = 2\pi\mu(k)$. The co-weights $\mu(k)$ are dual to the simple roots and define the corners of the fundamental domain of the $SU(N)$ algebra. They are defined in the adjoint representation $(\hat{T}_a)_{bc} = f_{abc}$ by

$$e^{-\hat{E}} = 1 , \quad \hat{E} = E_c \hat{T}_c \quad (37)$$

Here, mainly the gauge group $SU(2)$ will be considered, for which only one nontrivial center element $Z = -1$ exists, associated with the color structure

$$E = E_3 T_3 , \quad E_3 = 2\pi . \quad (38)$$

For the gauge group $SU(3)$, there are two nontrivial center elements

$$Z(1) = e^{i2\pi/3} , \quad Z(2) = e^{-i2\pi/3} \quad (39)$$

which are generated from (36) by the vectors $E(1)$ and $E(2)$, whose non-vanishing components explicitly read

$$E_8(1) = \frac{4\pi}{\sqrt{3}} , \quad E_3(2) = 2\pi , \quad E_8(2) = \frac{2\pi}{\sqrt{3}} . \quad (40)$$

Note that both vectors $E(1)$ and $E(2)$ satisfy the normalization

$$\text{tr}(E(k))^2 = -\frac{1}{2}E_c(k)E_c(k) = -\frac{8\pi^2}{3} \quad (41)$$

while

$$\text{tr}E(1)E(2) = -\frac{4\pi^2}{3} . \quad (42)$$

With (36), one has for the Wilson line along a path C in the vortex configuration (33)

$$W[\mathcal{A}](C) = Z(k)^{I(C,\Sigma)} \quad (43)$$

where

$$I(C, \Sigma) = \int_C dx_\mu \int_\Sigma d^{D-1}\tilde{\sigma}_\mu \delta^D(x - \bar{x}(\sigma)) \quad (44)$$

is the intersection number between C and Σ in D dimensions. For closed paths C , i.e. for Wilson loops, this equals the linking number between C and $S = \partial\Sigma$,

$$I(C, \Sigma) = L(C, S = \partial\Sigma) . \quad (45)$$

In particular, \mathcal{A} therefore satisfies the properties characterizing an ideal vortex configuration as formulated at the beginning of this section. As already mentioned in connection with eq. (27), the sheet Σ can be arbitrarily deformed by a (singular) Abelian gauge transformation, while keeping its boundary $S = \partial\Sigma$ fixed; this is entirely analogous to the lattice, where the stack of links $U = -1$ (in the case of $SU(2)$) forming the hypersurface Σ attached to the center vortex $S = \partial\Sigma$ can be deformed by center gauge transformations. A more explicit construction of this transformation is given further below in eq. (65).

On the other hand, in order to find a general representation of thin vortex configurations, consider the following gauge transformation,

$$V(k, \Sigma, x) = \exp(E(k)\Omega(\Sigma, x)) \quad (46)$$

where

$$\Omega(\Sigma, x) = \frac{1}{\omega_{D-1}} \int_\Sigma d^{D-1}\tilde{\sigma}_\mu \frac{\bar{x}_\mu(\sigma) - x_\mu}{(\bar{x}(\sigma) - x)^D} \quad (47)$$

is the solid angle taken up by the hypersurface Σ when viewed from x . Here,

$$\omega_{D-1} = \frac{2\pi^{D/2}}{\Gamma(D/2)} \quad (48)$$

is the area of the unit sphere S_{D-1} in D dimensions, so that the solid angle as defined above is normalized to unity for a point x inside a closed surface Σ . Note that the solid angle is defined with a sign depending on the orientation of Σ as rays emanating from x pierce Σ . A deformation of Σ keeping its

boundary $\partial\Sigma$ fixed leaves $\Omega(\Sigma, x)$ invariant unless x crosses Σ . In the latter case, $\Omega(\Sigma, x)$ changes by an integer.

For later convenience, note also that the solid angle (47) can be represented as

$$\Omega(\Sigma, x) = \int_{\Sigma} d^{D-1} \tilde{\sigma}_{\mu} \partial_{\mu}^x D(x - \bar{x}(\sigma)) \quad (49)$$

where $D(x)$ is the Green's function of the D -dimensional Laplacian,

$$- \partial_{\mu}^x \partial_{\mu}^x D(x - x') = \delta^4(x - x') . \quad (50)$$

For a closed surface $\Sigma = \partial M$ the solid angle agrees with the characteristic function $\chi(M, x)$ of M by Gauß' theorem,

$$\Omega(\Sigma, x) = \int_M d^D \sigma \delta^D(x - \bar{x}(\sigma)) = \chi(M, x) \quad (51)$$

i.e. any point inside $\Sigma = \partial M$ is associated with a solid angle 1, any point outside Σ with a vanishing solid angle,

$$\chi(M, x) = \begin{cases} 1 & x \in M \\ 0 & \text{otherwise} \end{cases} \quad (52)$$

In this respect, the normalized solid angle may also be interpreted as the linking number of the point x and the hypersurface Σ .

Consider now the gauge field induced by the gauge transformation (46) defined by the solid angle $\Omega(\Sigma, x)$,

$$V(k, \Sigma, x) \partial_{\mu} V^{\dagger}(k, \Sigma, x) = -E(k) \partial_{\mu} \Omega(\Sigma, x) . \quad (53)$$

Obviously, one has

$$\oint_C dx_{\mu} \partial_{\mu} \Omega(\Sigma, x) = 0 \quad (54)$$

for any closed curve C , so that any Wilson loop receives the trivial contribution

$$W[V \partial V^{\dagger}](C) = 1 . \quad (55)$$

Now one can show that indeed

$$V(k, \Sigma, x) \partial_{\mu} V^{\dagger}(k, \Sigma, x) = \mathcal{A}_{\mu}(k, \Sigma, x) - a_{\mu}(k, \partial\Sigma, x) \quad (56)$$

where a_{μ} and \mathcal{A}_{μ} are the thin and the ideal vortex fields, respectively, describing the same magnetic flux localized on $\partial\Sigma$. While \mathcal{A}_{μ} has already been

defined by eq. (33), an explicit representation for the thin vortex $a_\mu(k, \partial\Sigma, x)$ in (56) will be derived below. For this purpose, consider

$$\partial_\mu \Omega(\Sigma, x) = \int_\Sigma d^3 \tilde{\sigma}_\nu \partial_\mu \partial_\nu D(x - \bar{x}(\sigma)) \quad (57)$$

and write

$$\partial_\mu \partial_\nu = \delta_{\mu\nu} \partial^2 - (\delta_{\mu\nu} \partial^2 - \partial_\mu \partial_\nu) \quad (58)$$

i.e. express the longitudinal projector $L_{\mu\nu} = \partial_\mu \partial_\nu / \partial^2$ as $\delta_{\mu\nu} - \mathcal{P}_{\mu\nu}$, where $\mathcal{P}_{\mu\nu} = \delta_{\mu\nu} - \partial_\mu \partial_\nu / \partial^2$ is the transversal projector. Inserting this relation into eq. (57) and using the definition of the Green's function (50), one obtains

$$\partial_\mu \Omega(\Sigma, x) = - \int_\Sigma d^{D-1} \tilde{\sigma}_\mu \delta^D(x - \bar{x}(\sigma)) - \int_\Sigma d^{D-1} \tilde{\sigma}_\nu (\delta_{\mu\nu} \partial^2 - \partial_\mu \partial_\nu) D(x - \bar{x}(\sigma)) . \quad (59)$$

Upon inserting this relation into (53), the first term produces precisely the ideal vortex field $\mathcal{A}(k, \Sigma, x)$ as defined in eq. (33). To show that the second term yields the thin vortex field, it is necessary to express the transversal differential operator as

$$\delta_{\mu\nu} \partial^2 - \partial_\mu \partial_\nu = \frac{1}{2} \epsilon_{\mu\kappa\alpha\beta} \epsilon_{\nu\lambda\alpha\beta} \partial_\kappa \partial_\lambda . \quad (60)$$

After straightforward calculation, using Stokes' theorem, one eventually obtains

$$- \int_\Sigma d^{D-1} \tilde{\sigma}_\nu (\delta_{\mu\nu} \partial^2 - \partial_\mu \partial_\nu) D(x - \bar{x}(\sigma)) = - \int_{\partial\Sigma} d^{D-2} \tilde{\sigma}_{\mu\kappa} \partial_\kappa^{\bar{x}} D(x - \bar{x}(\sigma)) \quad (61)$$

Inserting this into eq. (53), one finds the thin vortex for arbitrary $\partial\Sigma$,

$$a_\mu(k, \partial\Sigma, x) = -E(k) \int_{\partial\Sigma} d^{D-2} \tilde{\sigma}_{\mu\kappa} \partial_\kappa^{\bar{x}} D(x - \bar{x}(\sigma)) \quad (62)$$

In Appendix A.2, it is shown explicitly that $a_\mu(k, \partial\Sigma, x)$ in eq. (62) indeed represents a center vortex, namely

$$\oint_C dx^\mu a_\mu(k, \partial\Sigma, x) = E(k) L(C, \partial\Sigma) \quad (63)$$

where $L(C, \partial\Sigma)$ is the linking number between C and $\partial\Sigma$.

Note that, unlike the ideal vortex $\mathcal{A}(\Sigma, x)$, the thin vortex $a(\partial\Sigma, x)$ depends only on the boundary $\partial\Sigma$, where the magnetic flux associated with the vortex is located.

It is now easy to see that a gauge transformation which deforms the singular sheet Σ_1 , describing an ideal vortex, into another sheet Σ_2 while keeping the boundary $\partial\Sigma$ fixed is given by

$$V(k, \Sigma_1, \Sigma_2, x) = V^{-1}(k, \Sigma_1, x)V(k, \Sigma_2, x) \quad (64)$$

$$= \exp[-E(k)(\Omega(\Sigma_1, x) - \Omega(\Sigma_2, x))] \quad (65)$$

Since the boundaries of Σ_1 and Σ_2 match, $\partial\Sigma_1 = \partial\Sigma_2$, the thin vortices arising from $V(\Sigma_1)\partial V^\dagger(\Sigma_1)$ and $V(\Sigma_2)\partial V^\dagger(\Sigma_2)$ cancel and one obtains

$$(\mathcal{A}(k, \Sigma_1, x))^{V(k, \Sigma_1, \Sigma_2, x)} = \mathcal{A}(k, \Sigma_2, x) . \quad (66)$$

One can also easily convince oneself that the transformation (65) agrees with the one introduced in section 3.2, eq. (26). Since $\Sigma_1 \cup (-\Sigma_2) = \partial M$ represents the closed orientable surface of some volume M , application of Gauß' theorem yields

$$\Omega(\Sigma_1, x) - \Omega(\Sigma_2, x) = - \int_{\Sigma_1} d^{D-1} \tilde{\sigma}_\mu \partial_\mu^{\bar{x}} D(x - \bar{x}(\sigma)) \quad (67)$$

$$+ \int_{\Sigma_2} d^{D-1} \tilde{\sigma}_\mu \partial_\mu^{\bar{x}} D(x - \bar{x}(\sigma))$$

$$= - \int_{\Sigma_1 \cup (-\Sigma_2)} d^{D-1} \tilde{\sigma}_\mu \partial_\mu^{\bar{x}} D(x - \bar{x}(\sigma)) \quad (68)$$

$$= \int_M d^D \tilde{\sigma} (-\partial_\mu^{\bar{x}} \partial_\mu^{\bar{x}}) D(x - \bar{x}(\sigma)) . \quad (69)$$

Using the definition of the Green's function of the D -dimensional Laplacian (50), one obtains

$$\Omega(\Sigma_1, x) - \Omega(\Sigma_2, x) = \int_M d^D \tilde{\sigma} \delta^D(x - \bar{x}(\sigma)) = \chi(M, x) \quad (70)$$

where $\chi(M, x)$ is the characteristic function of M defined in eq. (52), and $\partial M = \Sigma_1 \cup (-\Sigma_2)$. Hence, the gauge transformation (65) can be expressed as

$$V(k, \Sigma_1, \Sigma_2, x) = \exp[-E(k)\chi(M, x)] \quad (71)$$

$$= Z(k)^{\chi(M, x)} . \quad (72)$$

Thus, one recovers precisely the transformation already introduced in (26).

3.4 Continuum limit of the Maximal Center gauge

On the basis of the groundwork laid out in the previous sections, it is now straightforward to construct the analogue of the maximal center gauge for continuum Yang-Mills fields. The transformations $V(\Sigma)$ characterized by (18) allow to carry out precisely step 1.) of the maximal center gauge fixing procedure, as specified in section 2.3, in the continuum. Given an initial smooth gauge field A , the transformed field $A^{V(\Sigma)}$ contains ideal vortices described by hypersurfaces Σ of one's choice. Furthermore, in analogy to the lattice, where taking the coset part of a configuration amounts to leaving away all ideal vortices $\mathcal{A}(k, \Sigma, x)$, one can define the stripped configuration

$$(A^V)' = A^V - \mathcal{A}(k, \Sigma) = VAV^\dagger - a(k, \partial\Sigma) \quad (73)$$

with the thin vortex field a defined in terms of V as in (23) and (24), an explicit representation being given by eq. (62). This stripped configuration induces the same behavior for arbitrary Wilson line integrals as the configuration A^V , except for the center element jumps at the hypersurfaces Σ . In fact, $(A^V)'$ depends only on the thin vortex configuration a , with thin vortices at $\partial\Sigma$, and not on the specific choice of the entire hypersurface Σ , cf. eq. (28). It is therefore the precise analogue of the coset part in the lattice case. Note that $(A^V)'$ is still singular on $\partial\Sigma$.

According to step 2.) of the maximal center gauge fixing procedure as specified in section 2.3, one must now consider all coset gauge transformations of $(A^V)'$ such as to maximize the gauge fixing functional. As explained in the previous section, this step can be straightforwardly translated to the continuum, where gauge fields are subject to arbitrary local coset transformations. Expressing therefore the coset link configuration in the continuum limit, cf. eq. (17),

$$U'_\mu = 1 - lA'_\mu + \frac{l^2}{2}(A'_\mu)^2 - \dots \quad (74)$$

the maximal center gauge fixing condition (16) can be rewritten as

$$\max_{\Sigma} \max_G \int d^D x g \left(\text{tr} \left((A_\mu^{V(\Sigma)})'^G (A_\mu^{V(\Sigma)})'^G \right) \right) \quad (75)$$

where the arbitrary gauge fixing function has also been redefined,

$$g(t) = \frac{1}{l^D} \bar{g} \left(2 + \frac{l^2}{2} t \right) . \quad (76)$$

Like \bar{g} , g should be a monotonously rising function. Note that in (75), the maximization is, as written, over all hypersurfaces Σ , and not over all possible associated transformations $V(\Sigma)$. For every Σ , there are many possible $V(\Sigma)$. Only one $V(\Sigma)$ must be constructed and inserted in (75) for every choice of Σ .

Inserting (73), the gauge fixing condition can be written as

$$\max_{\Sigma} \max_G \int d^D x g \left(\text{tr} \left(GV(A - a)V^\dagger G^\dagger + G\partial G^\dagger \right)^2 \right). \quad (77)$$

This expression can be further simplified such as to eliminate all explicit reference to the singular transformations V . In the following calculation, there is a slight subtlety. Namely, the integrand in (77) is continuous at hypersurfaces Σ ; it was precisely constructed to be so. Thus, one may replace its value on hypersurfaces Σ by the limit as one approaches Σ . In the following, the integrand in (77) will therefore be evaluated outside of Σ and its value on Σ is then defined by continuity. In particular, this means that one may set $V\partial V^\dagger = -a$, cf. eq. (24).

By writing $G = V\bar{G}V^\dagger$, the argument of the gauge function g in (77) becomes

$$\text{tr} \left(V\bar{G}(A - a)\bar{G}^\dagger V^\dagger + V\bar{G}(V^\dagger\partial V)\bar{G}^\dagger V^\dagger + V(\bar{G}\partial\bar{G}^\dagger)V^\dagger + V\partial V^\dagger \right)^2 \quad (78)$$

$$= \text{tr} \left(V\bar{G}A\bar{G}^\dagger V^\dagger + V(\bar{G}\partial\bar{G}^\dagger)V^\dagger + V\partial V^\dagger \right)^2 \quad (79)$$

$$= \text{tr} \left(VA\bar{G}V^\dagger - a \right)^2 \quad (80)$$

$$= \text{tr} \left(A\bar{G} - a \right)^2 \quad (81)$$

where the fact that V and a commute was used. Note that \bar{G} is continuous on Σ , since it is quadratic in V and hence insensitive to the center phase V picks up at hypersurfaces Σ . Thus, it can still be considered a coset gauge transformation. Vice versa, any coset transformation \bar{G} is associated with a coset transformation G . Therefore, the gauge fixing condition (77) can be rewritten as

$$\max_{\Sigma} \max_{\bar{G}} \int d^D x g \left(\text{tr} \left(A\bar{G} - a \right)^2 \right) \quad (82)$$

with the coset maximization running over all coset transformations \bar{G} .

In this form, maximal center gauge fixing is revealed more clearly as an approximation problem in the mathematical sense; it corresponds to approximating the gauge orbit of a given gauge configuration A as well as possible

by thin vortex configurations a . The precise metric defining how close a thin vortex field a is to the gauge orbit of A is encoded in the arbitrary function g . Thus, the continuum formulation of the maximal center gauge provides a deeper understanding of the empirical fact drawn from lattice experiments [10], namely that center projection vortices provide a rough localization of thick vortex structures present in full lattice Yang-Mills field configurations. Note that, in mathematical terms, the space of thin vortex fields a has no scalar product or orthogonality properties. Eq. (82) specifies a norm which serves to define an approximation problem within this space, namely maximal center gauge fixing.

Note that the gauge fixing functional (82) only depends on the thin vortex configuration a , with vortices localized on $\partial\Sigma$, and not on the whole choice of Σ . This is the continuum counterpart of the lattice observation that the maximal center gauge leaves the center of the gauge group unfixed, i.e. does not depend on the center part of a configuration.

As a last step, it is interesting to recast the coset gauge fixing condition in differential form as follows. Consider Σ and an associated thin vortex field $a(\partial\Sigma)$ as given. Then a gauge field A satisfies the condition of providing the maximal value of the gauge fixing functional under the action of arbitrary coset transformations \tilde{G} if the value of the gauge fixing functional (82) is stationary under infinitesimal transformations $\tilde{G} = \exp(-\theta) \approx 1 - \theta$,

$$0 = \frac{\delta}{\delta\theta^a(y)} \int d^D x g \left(\text{tr} ([A, \theta] + \partial\theta - a)^2 \right) \quad (83)$$

$$= \int d^D x g' \left(\text{tr}(A - a)^2 \right) (A^c - a^c) (-\partial\delta^{ac} - A^d f^{dac}) \delta^D(x - y) \quad (84)$$

$$= \partial_\mu \left[g' \left(\text{tr}(A - a)^2 \right) (A_\mu^a - a_\mu^a) \right] - g' \left(\text{tr}(A - a)^2 \right) f^{adc} A^d a^c \quad (85)$$

where the prime on g denotes the derivative with respect to the argument. By multiplying with generators T_a , this reduces to

$$0 = F[A, a] = 2g'' \left(\text{tr}(A - a)^2 \right) \cdot \text{tr} \left((A_\nu - a_\nu) \partial_\mu (A_\nu - a_\nu) \right) \cdot (A_\mu - a_\mu) \\ + g' \left(\text{tr}(A - a)^2 \right) \left([\partial_\mu + a_\mu, A_\mu] - \partial_\mu a_\mu \right) \quad (86)$$

In the simple case $g(t) = t$, the gauge condition simplifies to

$$[\partial_\mu + a_\mu, A_\mu] - \partial_\mu a_\mu = 0 \quad (87)$$

If one in particular chooses the thin vortex configuration to satisfy the Landau gauge, $\partial_\mu a_\mu = 0$, then this condition is nothing but the background gauge

with the background given by the thin vortex field a . Note that the thin vortex configuration (62) satisfies the Landau gauge, as can be inferred from eq. (61).

Furthermore, if one has picked out of the gauge orbit of a given configuration A the element $A[a]$ which satisfies (86) for fixed arbitrary a (coset gauge fixing), then the remaining part of the maximal center gauge fixing procedure, i.e. finding the optimal a , reduces to solving

$$\max_{\Sigma} \int d^D x g \left(\text{tr}(A[a] - a)^2 \right) . \quad (88)$$

As mentioned repeatedly above, all choices of Σ in (88) corresponding to the same $\partial\Sigma$ are degenerate due to the unfixed center part of the $SU(2)$ gauge freedom. Also, for every $\partial\Sigma$, it is only necessary to construct one particular $a(\partial\Sigma)$, cf. the discussion after eq. (76).

Finally, having obtained an optimal hypersurface Σ , *center projection* simply means replacing the full gauge field by the corresponding ideal vortex configuration $\mathcal{A}(\Sigma)$, cf. eq. (33). This center projected configuration can then e.g. be used to evaluate observables such as the Wilson loop, cf. eq. (43).

3.5 Remarks on the center gauges in continuum Yang-Mills theory

3.5.1 Revisiting the thick vortex

In general, the gauge fixing condition (86) is not solvable by analytical means; at this stage, the value of the continuum formulation of the maximal center gauge lies more on a conceptual than on a practical level. However, it is worthwhile to briefly reexamine some properties of the examples presented in section 2.2 in the lattice framework. Namely, consider approximating (the gauge orbit of) a given thick $SU(2)$ vortex configuration centered on the origin of a two-dimensional space-time plane, cf. eq. (10),

$$A = T_3 \frac{f(\sqrt{x^2 + y^2})}{x^2 + y^2} (y\mathbf{e}_x - x\mathbf{e}_y) , \quad \partial A = 0 \quad (89)$$

by a thin vortex centered at the point $x_0\mathbf{e}_x$,

$$a = T_3 \frac{1}{(x - x_0)^2 + y^2} (y\mathbf{e}_x - (x - x_0)\mathbf{e}_y) \quad (90)$$

where the offset x_0 is still to be varied; $\mathbf{e}_x, \mathbf{e}_y$ denote the Cartesian unit vectors in the plane. For definiteness, the following treatment was carried out using a profile function $f(r) = \theta(r - R)$, i.e. a ring-shaped thick vortex of radius R similar to the one considered in section 2.2. In the case $x_0 = 0$, the gauge condition (86) is satisfied by these configurations, for arbitrary gauge fixing function g . For $x_0 \neq 0$, the condition (86) is in general not satisfied. Nevertheless, in terms of the variational form (82) of the gauge fixing condition, one has the relation

$$\int d^D x g (\text{tr}(A - a)^2) \leq \max_{\bar{G}} \int d^D x g (\text{tr}(A^{\bar{G}} - a)^2) \quad (91)$$

where equality is guaranteed for $x_0 = 0$. Now, it is possible to find gauge fixing functions g , e.g. $g = -\tanh(R^4 t^2)$, for which the quantity

$$\int d^D x g (\text{tr}(A - a)^2) \quad (92)$$

appearing on the left hand side of (91), viewed as a function of x_0 , exhibits a minimum at $x_0 = 0$. In view of (91), this implies that also the quantity on the right hand side,

$$\max_{\bar{G}} \int d^D x g (\text{tr}(A^{\bar{G}} - a)^2) \quad (93)$$

exhibits a minimum at $x_0 = 0$ (remember that equality is guaranteed in (91) for $x_0 = 0$). Therefore, according to the variational form of the gauge fixing condition (82), the optimal location of the approximating thin vortex configuration a , parametrized by x_0 , is achieved for $x_0 \neq 0$. This confirms the phenomenon observed in the lattice examples in section 2.2, that the thin vortex induced by applying the center gauge fixing procedure to a radially symmetric thick vortex configuration does not necessarily appear concentrically with the original thick vortex. This property thus does not constitute a lattice artefact, but persists also in the continuum theory.

As a final remark, note that the simple choice of gauge fixing function $g(t) = t$ leads to a trivial optimal thin vortex configuration $a = 0$ for any smooth initial configuration A . This is due to the fact that a thin vortex field diverges as $1/r$, where r is the distance from the vortex, and therefore $\text{tr}(A - a)^2$ diverges as $-1/r^2$ at the positions of the thin vortices. Therefore, in the case $g(t) = t$, the only choice of thin vortex field which does not render the gauge fixing functional (88) divergent is $a = 0$. Consequently, $a = 0$ trivially turns out to be the optimal thin vortex approximation, for any smooth $A_\mu(x)$. The

choice $g(t) = t$ for the gauge fixing function thus at first sight does not seem very useful, since it cannot lead to a faithful representation of the vortex content of the original smooth gauge field A . The same is true for any $g(t)$ which diverges as fast as, or faster than, $g(t) = t$ as $t \rightarrow \infty$.

3.5.2 Remarks on the Direct Maximal Center Gauge

The choice of gauge fixing function $g(t) = t$ is the continuum analogue of a variety of lattice gauge fixing functions $\bar{g}(x)$, cf. eq. (76) in the limit $l \rightarrow 0$. Among these is the case $\bar{g}(x) = x^2$ (after leaving away irrelevant constants). This is the standard “Direct Maximal Center Gauge” [18],[21],[25]. Strictly speaking, therefore, this gauge does not have a useful continuum limit on the level of gauge fixing individual smooth continuum gauge field configurations. The question arises how this gauge leads to a finite center projection vortex density in the continuum limit of the lattice formulation, as evidenced by the renormalization group scaling behavior of this density [20] (note erratum in [11]), see also [21]. Several possible explanations come to mind.

For one, in a lattice calculation, one never takes the continuum limit of the field configurations at an intermediate stage. Instead, one operates with regularized lattice configurations and only extrapolates observables at the end of the calculation to the continuum limit. Thus, on the lattice, one always stays away a certain minimal distance from the $1/r$ -singularity of the continuum thin vortex, i.e. one never probes the $t \rightarrow \infty$ behavior of $g(t)$. More precisely, one cannot make a distinction between $g(t) = t$ and a “capped” version $g_T(t) = t\theta(T-t) + T\theta(t-T)$, with a sufficiently large value of T . Of course, as the lattice spacing is taken to zero, T will have to diverge if g and g_T are to remain equivalent. Now, it is entirely possible that the choice $g(t) = t$ leads to scaling violations of the projection vortex density on very fine lattices, such that this density ultimately tends to zero. On the other hand, a capped version $g_T(t)$ as above, with large but fixed T , allows a finite projection vortex density for smooth continuum configurations. Possibly, present lattices are still too coarse to reveal the above scaling violations and distinguish between $g(t) = t$ and $g_T(t)$ with large fixed T . An observation which supports this possibility is that on present lattices, one still finds in typical configurations an abundance of negative plaquettes, i.e. structures indistinguishable from thin vortices on the scale of the lattice spacing. On the other hand, the appeal of this explanation is lessened by the fact that it calls into question the relevance of the scaling behavior observed for the projection

vortex density; usually, such behavior is considered a firm indication that the continuum limit of an observable can be extrapolated with confidence.

A second explanation can be based on the fact that functional integrals in field theory are dominated, for entropy reasons, by configurations with infinite action, not by smooth configurations [27]. For instance, if typical configurations A contain thin vortices, despite the fact that they are associated with a divergent Yang-Mills action, then in the process of maximal center gauge fixing, i.e. approximating the configurations by thin vortices, one would indeed introduce a nontrivial thin vortex configuration a to cancel all thin vortices in the combination $A - a$. This would happen also for the choice of gauge fixing function $g(t) = t$. However, it has been argued that thin vortices are too singular to survive the continuum limit of lattice Yang-Mills theory [17]. In this simple form, this second explanation is therefore questionable.

However, a third explanation which is a slightly more sophisticated variant of the second one is possible. When fixing to the maximal center gauge on the lattice, one never finds the exact maximum of the gauge fixing functional, but only an approximation of this maximum. Put another way, consider introducing the (negative) gauge fixing functional as a weight into the Yang-Mills partition function,

$$S_{GF} = -q \int d^D x g \left(\text{tr}(A[a] - a)^2 \right) \quad (94)$$

cf. eq. (88). Then, in practice, one does not insist on the limit $q \rightarrow \infty$, which would imply finding the exact minimum of S_{GF} ; instead one may be satisfied with a finite value of q . In this case, a competition between the gauge fixing term and the Yang-Mills action (and also a competition between different Gribov copies, i.e. relative minima of S_{GF}) becomes possible. Even in a case such as $g(t) = t$, where the gauge fixing term in general will diverge for nontrivial thin vortex configurations a , these divergences may be swamped by the infinite action of typical Yang-Mills field configurations. Note that for this to work, only Yang-Mills configurations considerably less singular than the thin vortices invoked in the second explanation above are necessary. E.g., in the case of the gauge fixing function $g(t) = t$, the gauge fixing term for a nontrivial thin vortex configuration a will diverge as $\int dr r(1/r^2)$, where r denotes the distance from the thin vortex. This is independent of the dimension of space-time; the coordinates perpendicular to a vortex always span two dimensions. On the other hand, in four space-time dimensions,

already a gauge field configuration which behaves as $1/r$ in the vicinity of a point singularity will induce an action diverging as $\int dr r^3(1/r^4)$; a divergence of the same degree is induced by a $1/\sqrt{r}$ line singularity or a $\ln(r)$ sheet singularity in four space-time dimensions.

3.5.3 Alternative vortex gauges

The remarks above illustrate that the continuum maximal center gauge in the form derived in section 3.4 in a sense constitutes excessive rigor. In a *dynamical* calculation, one is forced to introduce a regularization of divergences in the ultraviolet; this regularization in particular also smears out the thin vortex configurations $a(\partial\Sigma)$, used in maximal center gauge fixing, into thick vortices with a thickness related to the ultraviolet cutoff. In view of this regularization, dictated by the dynamics, it is not mandated to consider at an intermediate stage the behavior of gauge field configurations as the cutoff is removed. Instead, the cutoff must be kept finite throughout the calculation, and only the continuum limit of physical observables, as encoded in their renormalization group behavior, is relevant.

This suggests an alternative formulation of the gauge fixing procedure in which one approximates a given gauge configuration as well as possible by thick vortices. Specifically, one can generalize the gauge condition (86) and the remaining maximization problem (88) by allowing the approximating configurations $a(\partial\Sigma)$ to comprise thick vortices. Of course, such a generalization clouds the original idea of the maximal center gauge, namely keeping the center part of the gauge freedom on the lattice unfixed; instead, it operates purely with continuum, i.e. coset configurations. Therefore, such gauges should be more appropriately called maximal vortex gauges rather than center gauges.

In such vortex gauges, one has an additional freedom in the choice of the thickness of the approximating vortex configurations $a(\partial\Sigma)$. On the one hand, one may choose the thickness to be related to the ultraviolet cutoff with which one regulates the theory; for example, the thickness may simply be the lattice spacing. This form would be entirely equivalent to the maximal center gauge in the lattice theory, since, at the level of the regularized theory, there is no distinction between such a thick vortex and a truly thin one. On the other hand, one may choose the thickness to be a fixed physical quantity¹⁰

¹⁰Some phenomenological implications of a physical vortex thickness were discussed in [23],[24].

(which can be varied to optimally match the vortex profile preferred by the Yang-Mills dynamics). In this form, the thick vortex profile can also take over the role of the gauge fixing function g . For example, as evidenced in the examples given further above, the gauge fixing function g can act as a regulator for the divergences introduced into the gauge fixing functional by the singularities of the thin vortices. In a vortex gauge with thick vortices, this is already achieved by the vortex thickness. In many respects, the vortex profile in the vortex gauge has a similar effect as the gauge fixing function g in the maximal center gauge.

As an aside, note that in a consistently regularized theory, one should also use regularized versions of the ideal vortex configurations \mathcal{A} , cf. (33), which one simply obtains by using the ultraviolet cutoff of the theory to smooth out the δ -functions in (33), cf. eq. (133).

Lastly, a certain aspect of continuum thin (or, equivalently, ideal) vortices has not yet been discussed in detail, namely the possibility that there may exist distinct thin vortex fluxes which contribute an identical phase to any Wilson loop they link. An example of this was given already in section 2.2; in the $SU(2)$ thin vortex configuration, eq. (9),

$$a_\varphi = \pm \frac{1}{r} T_3, \quad a_r = 0 \tag{95}$$

both choices of sign lead to the same effect on a linked Wilson loop. Both choices correspond to a Cartan chromomagnetic flux described by $E_3 = 2\pi$, cf. eq. (38), but they differ in the direction, or orientation, of the flux, which is inverted when the sign is reversed.

On the other hand, on a $Z(2)$ lattice, one cannot distinguish between these two possibilities, since one formulates the theory directly in terms of group elements. On a $Z(2)$ lattice, there is only one type of center vortex flux, defined by plaquettes taking the value (-1) . Information about the orientation of the flux is lost during lattice center projection. For the purpose of evaluating Wilson loops, this is immaterial; however, there may be other observables which are sensitive to the orientation of vortex flux. An important example of this, namely the Pontryagin index, will be discussed in detail in section 5.

Thus, to obtain a comprehensive description of infrared phenomena in Yang-Mills theory, it is necessary to project onto a slightly more general class of infrared effective degrees of freedom than the essentially unoriented center

vortices defined by lattice center projection. Namely, vortex surfaces should additionally be associated with an orientation, and should in general consist of patches of differing orientation. As will be shown in section 5 in detail, the edges of these patches can be associated with Abelian magnetic monopole trajectories. The continuum center vortices introduced in the past sections do already include information about the orientation of magnetic flux. E.g., in the discussion after eq. (76), when maximization over all hypersurfaces Σ is called for, different orientations of Σ can be used. Likewise, in the discussion after eq. (88), different orientations of $\partial\Sigma$, i.e. directions of flux in a , are distinguishable. However, vortex surface patches of alternating orientation, bounded by Abelian monopole currents, have hitherto not been allowed. On the contrary, the magnetic flux carried by thin vortex configurations a has been assumed to be continuous throughout.

The purpose of the the present discussion is merely to round out the treatment of maximal center gauge fixing and center projection by pointing out how it can easily be generalized to yield vortex surfaces made up of oriented patches. More detailed properties of such surfaces, including how they determine the Pontryagin index, are discussed in section 5.

One way of introducing patches of different orientation on the vortex surfaces is to include information on Abelian monopole degrees of freedom into the gauge fixing and projection procedure. As mentioned above, the trajectories of such monopoles on vortex surfaces define the edges of the oriented patches. Such a procedure has already been defined and implemented in the lattice formulation, namely the “Indirect Maximal Center Gauge” introduced in [10] and further investigated in [18]. This procedure is defined by initially transforming a given lattice Yang-Mills configuration to the maximal Abelian gauge and performing Abelian projection, which allows to extract Abelian monopole trajectories. In a subsequent step, one transforms the residual Abelian lattice configuration to the maximal center gauge and performs center projection, allowing the extraction of vortex surfaces. This two-step procedure, including two truncations of the theory by projection, is easily translated into the continuum formulation; the maximal Abelian gauge corresponds to the gauge fixing condition

$$[\partial_\mu + A_\mu^{(n)}, A_\mu^{(ch)}] = 0 \tag{96}$$

where $A_\mu^{(n)}$ denotes the color neutral (Cartan) components of the gauge field, and $A_\mu^{(ch)}$ denotes the color charged components. Fixing to this gauge induces

Abelian monopoles in the resulting field configurations. After projecting the gauge-fixed configurations onto their color neutral part (Abelian projection), the maximal center gauge fixing procedure, as described in the past sections, can be implemented analogously, and the associated vortices extracted.

Note that the construction does not guarantee a priori that the monopoles are located on the vortex surfaces. However, monopoles have been found empirically to lie on the center vortices extracted via the indirect maximal center gauge in lattice experiments [18].

On the other hand, it is not strictly necessary to resort to such a two-step procedure, one of the steps being geared to extract Abelian monopoles, and the other to extract center vortices. The coset gauge transformations \bar{G} in the maximal center gauge fixing functional (82) in particular include gauge transformations which generate Dirac strings¹¹. Dirac strings, which describe open two-dimensional world-sheets in four-dimensional space-time, carry quantized magnetic flux such that they do not influence any Wilson loop, in accordance with the fact that they are unobservable pure gauge artefacts. E.g., in the case of $SU(2)$ color, a Dirac string carries twice the magnetic flux of a thin vortex. Before discussing the interplay between vortices and Dirac strings, consider the following example for illustration. The $SU(2)$ pure gauge configuration

$$a^{dirac} = \bar{G}\partial\bar{G}^\dagger, \quad \bar{G} = \begin{pmatrix} \cos(\theta/2) & \sin(\theta/2)e^{-i\varphi} \\ -\sin(\theta/2)e^{i\varphi} & \cos(\theta/2) \end{pmatrix} \quad (97)$$

where (r, θ, φ) denotes the usual three-dimensional spherical coordinates, and the configuration may be considered constant in the further space-time coordinate, has the explicit components

$$a_r^{dirac} = 0, \quad a_\theta^{dirac} = \frac{1}{2r} \begin{pmatrix} 0 & -e^{-i\varphi} \\ e^{i\varphi} & 0 \end{pmatrix} \quad (98)$$

$$a_\varphi^{dirac} = \frac{i}{r \sin\theta} \sin(\theta/2) \begin{pmatrix} \sin(\theta/2) & \cos(\theta/2)e^{-i\varphi} \\ \cos(\theta/2)e^{i\varphi} & -\sin(\theta/2) \end{pmatrix} \quad (99)$$

¹¹Note that the description in terms of Dirac strings, used in the following for convenience, is equivalent to a description in terms of Abelian monopoles. The two objects are strictly coupled. Monopole trajectories define the edges of Dirac string world-sheets; Dirac string world-sheets span areas circumscribed by monopole trajectories, where the specific area associated with a monopole trajectory can be modified by gauge transformations.

The full nonabelian field strength of this configuration can easily be verified to vanish [28], except on the negative z -axis¹², i.e. for $\theta = \pi$. There, the Dirac string is located. For $\theta \rightarrow \pi$, a_φ^{dirac} can be approximated by

$$a_\varphi^{dirac} \approx -\frac{1}{r \sin \theta} \cdot 2T_3 = 2a_\varphi^{thin \text{ vortex}} \quad (100)$$

and the flux through an infinitesimal Wilson loop encircling the Dirac string therefore is

$$\Phi = \int_0^{2\pi} d\varphi r \sin \theta a_\varphi^{dirac} = -4\pi T_3 \quad (101)$$

leading, upon exponentiation, to the trivial value $W = 1$ for the Wilson loop. Furthermore, by considering the Abelian projection \bar{a}^{dirac} of a^{dirac} ,

$$\bar{a}_\varphi^{dirac} = \frac{-2 \sin^2(\theta/2)}{r \sin \theta} T_3, \quad \bar{a}_\theta^{dirac} = \bar{a}_r^{dirac} = 0, \quad (102)$$

one obtains in the associated Abelian magnetic field

$$\bar{B} = \partial \times \bar{a}^{dirac} = -\frac{1}{r^2} e_r T_3 \quad (103)$$

a Dirac magnetic monopole located at the boundary of the Dirac string. Note that in the full field strength, this field is completely canceled by the nonabelian part [28], as mentioned above. Thus, magnetic monopoles which become visible in Abelian-projected configurations can be used as an alternative way of detecting, or describing, the Dirac strings induced by coset gauge fixing.

The above properties imply that a Dirac string world-sheet which coincides with a (oppositely oriented) patch of a thin $SU(2)$ vortex world-sheet simply reverses the magnetic flux associated with that patch, leaving all Wilson loops invariant. Nevertheless, in this way, though representing a pure gauge on its own, a Dirac string may change what information contained in a configuration is kept during continuum center (or vortex) projection, i.e. it can be used to define a different truncation of the theory. The physical content of the full configurations of course is not influenced by the Dirac string.

It should be noted that for higher $SU(N)$ color groups, the superposition of a Dirac string on a vortex changes not only the sign (i.e. the orientation),

¹²The action of this pure gauge configuration of course must vanish in spite of the singularity on the negative z -axis, cf. the pertinent comments in Appendix A.1.

but in general also the type of vortex flux, i.e. its direction in color space. E.g. for $SU(3)$, one in general additionally exchanges the center flux labels $(k = 1) \leftrightarrow (k = 2)$ in eq. (40). This happens precisely in such a way as to leave all Wilson loops invariant, as it should be.

Thus, due to the possibility of vortex surfaces being partially covered by Dirac string world-sheets generated by coset transformations \tilde{G} in (82), vortex surfaces made up of patches of different orientation are automatically generated during continuum center gauge fixing. Vortex projection must merely be generalized to include this additional information about the orientation of vortex magnetic flux resulting from the Dirac world-sheets generated by coset gauge fixing.

Finally, it should be noted that thick analogues of vortex surfaces consisting of patches of different orientation have been constructed in [29],[30]. Using such generalized objects as approximating configurations a in the gauge fixing condition (82) provides another, alternative, way of extracting information about vortex orientation from gauge field configurations.

4 Sketch of an Effective Vortex Theory

The center dominance observed for the string tension in lattice Monte Carlo calculations using the maximal center gauge [18],[21],[10],[11],[12] supports the notion that center vortices are the infrared degrees of freedom relevant for confinement in Yang-Mills theory. On a formal level, center or vortex dominance implies that the confinement properties can be adequately described by an effective vortex theory which results by appropriately integrating out all other Yang-Mills degrees of freedom. More specifically, in the abovementioned lattice calculations, center dominance is obtained using the full lattice Yang-Mills dynamics, i.e. the field configurations are sampled according to the full Yang-Mills action. Center projection is only performed in the observable, i.e. the Wilson loop is evaluated using center-projected configurations after maximal center gauge fixing. Thus, in principle, one could evaluate the expectation value of the Wilson loop using a $Z(N)$ effective action obtained after integrating out all coset $SU(N)/Z(N)$ degrees of freedom. In lattice calculations, this separation of the functional integrations is impractical, and the $Z(N)$ effective action is unknown.

Adopting a continuum description does not greatly alleviate this problem, and therefore the following considerations concerning the effective theory of

vortices must remain mostly on a formal level. The intention is to sketch what types of effects may arise in the effective vortex theory particularly in the long-wavelength domain.

To this end, it is necessary to implement a maximal center gauge in the Yang-Mills functional integral. This gauge fixing can be decomposed into two steps, as shown in section 3.4, namely coset gauge fixing in an arbitrary fixed thin vortex configuration a and optimization of the thin vortex configuration. Coset gauge fixing can be achieved in the standard way via the Fadeev-Popov procedure, i.e. the gauge fixed partition function takes the form

$$Z = \int [DA] \Delta_F[A, a] \exp \left(-S_{YM}[A] - pF^2[A, a] \right) \quad (104)$$

where $F[A, a]$ denotes the gauge fixing condition (86), $\Delta_F[A, a]$ is the standard Fadeev-Popov determinant corresponding to this gauge fixing condition, and p is a gauge fixing parameter which should be sent to infinity in order to implement the coset gauge fixing condition (86) exactly. Note that at this point a is an arbitrary, but fixed, external (thin vortex) field configuration. In order to optimize the choice of thin vortex field a , it is useful to further introduce into the functional integral the following representation of unity¹³,

$$1 = \Delta[A] \int [D\Sigma] \exp \left(-S_{GF}[A, a(\partial\Sigma)] \right) \quad (105)$$

$$S_{GF} = -q \int d^D x g \left(\text{tr}(A - a)^2 \right) \quad (106)$$

cf. eq. (88). Here, the integration runs over all $(D - 1)$ -dimensional hypersurfaces Σ in D space-time dimensions, and the specific realization $a(\partial\Sigma)$ of a thin vortex on $\partial\Sigma$ can e.g. be given by (62). Furthermore, the gauge fixing parameter q should also be sent to infinity in order for $e^{-S_{GF}}$ to be peaked at the optimal thin vortex configuration.

Note that (105), in order to be properly defined, at the very least requires some further gauge fixing due to the fact that the integrand depends only on the boundaries $\partial\Sigma$ of the hypersurfaces Σ being integrated over. Note that it is by no means clear that the integral over hypersurfaces Σ can simply be replaced by an integral over closed surfaces S ; there may exist closed surfaces S which cannot be represented as $S = \partial\Sigma$ in terms of some hypersurface Σ .

¹³Note that one could also forego separating coset gauge fixing and vortex optimization, and instead use the full continuum maximal center gauge fixing functional (82) to introduce a representation of unity into the Yang-Mills functional integral analogously to (105).

A simple example is one of the coordinate planes, e.g. the 1-2-plane, in a four-dimensional space-time hypercube endowed with periodic boundary conditions, i.e. a torus. Such a plane constitutes a closed surface due to the periodic boundary conditions, but cannot be represented as the boundary of any three-volume Σ . In general, the number of topologically inequivalent closed two-dimensional surfaces which are not boundaries of three-volumes is given by the dimension of the 2nd homology group $H_2(M)$ of the space-time manifold M under consideration; this corresponds to the 2nd Betti number $b_2 = \dim H_2(M)$. On the four-dimensional torus T^4 , one has $b_2(T^4) = 6$, corresponding precisely to the six independent planes which are closed by the periodic boundary conditions.

Formally, one can e.g. modify (105) by writing

$$1 = \bar{\Delta}[A] \int [DS] \int [D\Sigma] \delta[\Sigma - \Sigma_{min}[S]] \exp(-S_{GF}[A, a(S)]) \quad (107)$$

where $\Sigma_{min}[S]$ denotes the hypersurface of minimal volume which has S as its boundary, $\partial\Sigma_{min} = S$. If no hypersurface Σ exists such that $\partial\Sigma = S$, then that S does not contribute in (107). Note that this modification, leaving from the original integration over hypersurfaces Σ only an integration over closed $(D - 2)$ -dimensional surfaces S in D space-time dimensions, corresponds precisely to a fixing of the center part of the gauge freedom on the lattice. Note also that this further gauge fixing in general leads to further measure factors, cf. the modified measure $\bar{\Delta}[A]$ in (107) as opposed to $\Delta[A]$ in (105).

Inserting (107) into (104), and assuming functional integrations can be interchanged, one arrives at

$$Z = \int [DS] e^{-S_{eff}[S]} \quad (108)$$

$$e^{-S_{eff}[S]} = \int [D\Sigma] \delta[\Sigma - \Sigma_{min}[S]] \cdot \int [DA] \bar{\Delta}[A] \Delta_F[A, a] e^{-S_{YM}[A] - pF^2[A, a] - S_{GF}[A, a]} \quad (109)$$

where $a \equiv a(S)$, as specified e.g. by (62). The effective action given by (109) describes a theory of $(D - 2)$ -dimensional closed vortex surfaces S in D space-time dimensions. In the most general case, e.g. for the purpose of evaluating the vortex-projected Pontryagin index, cf. next section, one will supplement the surfaces S with information about Dirac strings contained

in the coset gauge-fixed configurations A ; this leads to patches of different orientation on S as indicated in section 3.5.3. Formally, the surfaces S being integrated over in (108) will consist of oriented patches, and the integration over A in (109) for given S will in turn be restricted to all A containing the corresponding Dirac string configuration.

Of course, the previous manipulations are at this stage purely formal. Even to obtain the measure $\bar{\Delta}[A]$ in (109), one has to solve a string theory in an arbitrary gauge background A in four space-time dimensions, namely one has to carry out the integral over S in (107). However, in lower dimensions, an evaluation of (107) may be feasible. E.g., in three space-time dimensions, the S denote closed lines, and the integration over S may be converted to a field theory by interpreting these lines as world-lines of particles.

In order to nevertheless gain some insight into the structure of the vortex effective action at least in the infrared limit, assume the validity of the statement that the center projection vortices in Yang-Mills theory give a rough localization of thick vortices present in the full Yang-Mills configurations. As discussed in section 2.2, this statement is corroborated by empirical findings in lattice experiments [10] and can be understood on the basis of the continuum formulation of the maximal center gauge developed in section 3. However, it is a statement which can at most be considered valid on length scales coarser than the typical thickness R of the aforementioned vortices in the full configurations preferred by the Yang-Mills dynamics. At this point, R is an undetermined scale; it should ultimately be extracted by minimizing the effective thick vortex action, as indicated further below.

The above statement implies that the distribution of thin projection vortex configurations in the infrared regime is simply determined by the distribution of thick vortices in Yang-Mills theory. In other words, the infrared effective action of projection vortices can be obtained by calculating the standard Yang-Mills effective action of thick vortex configurations, using a thick vortex background gauge as already briefly discussed in section 3.5.3. The ultraviolet limit of validity of this effective action is given by the cutoff $\Lambda = 1/R$.

Furthermore, in such a long-wavelength approximation scheme, it is consistent to evaluate the effective action in a gradient expansion, i.e. in powers of $R\partial_i$, where $\partial_i \equiv \partial/\partial\sigma_i$ is the derivative with respect to the parameters of the vortex surface. Below, this effective action will be given in the classical limit, i.e. to zeroth order in a loop expansion. This will already exhibit the

relevant terms, with higher orders in the loop expansion only renormalizing the coefficients. The calculation is carried out explicitly in Appendix A.1 using, for convenience, ultraviolet-regulated ideal vortex configurations. More precisely, the δ -function in the defining expression (33) for the ideal vortex $\mathcal{A}(k, \Sigma, x)$ is regularized by means of the cutoff $\Lambda = 1/R$, cf. eq. (133). Note that such an object represents a bona fide thick vortex; the special character of ideal vortices as singular continuum representations of excitations on a $Z(N)$ lattice is blurred when the ideal vortex singularities are regularized. After regularization, there is no qualitative distinction between an initially thin or an initially ideal vortex; these can all be viewed as continuum coset configurations, namely, thick vortices.

Inserting such a thickened ideal vortex \mathcal{A} into the classical Yang-Mills action,

$$S[\mathcal{A}] = -\frac{1}{2g_0^2} \int \text{tr} (F[\mathcal{A}]F[\mathcal{A}]) \quad (110)$$

one obtains the gradient expansion (see Appendix A.1)

$$\begin{aligned} S_{YM}[\mathcal{A}] = & \alpha \int_{\partial\Sigma} d^2\sigma \sqrt{g} + \beta \int_{\partial\Sigma} d^2\sigma \sqrt{g} K_{ai}^A K_{bj}^A g^{ab} g^{ij} \\ & + \gamma \int d^2\sigma \sqrt{g} g^{ab} \partial_a \partial_b \ln \sqrt{g} . \end{aligned} \quad (111)$$

Here,

$$g = \det g_{ab} , \quad g_{ab} = \partial_a x^\mu \partial_b x^\mu \quad (112)$$

denotes the metric on the vortex sheet and K_{ab}^A are the extrinsic curvature coefficients which are defined in Appendix A.1, eq. (138). Furthermore, the coefficients in eq. (111) are given for $SU(2)$ vortices by (using $\text{tr} E^2 = -\frac{1}{2}(2\pi)^2$, cf. eq. (38))

$$\alpha = \frac{\pi}{g_0^2 R^2} , \quad \beta = -\frac{\pi}{2g_0^2} , \quad \gamma = \frac{\pi}{4g_0^2} . \quad (113)$$

One thus obtains in leading and next-to-leading order the Nambu-Goto action and curvature terms for the vortex surfaces¹⁴. The coefficients (113) will be renormalized through quantum effects embodied by higher orders in the loop expansion. In particular, renormalization will generate a physical scale in the coefficients in the standard fashion, which will allow to relate the thickness R to physically measurable quantities. This will make it possible to self-consistently determine the preferred physical vortex thickness R through a

¹⁴The second term on the r.h.s. of eq. (111) has been discussed in [31],[32].

minimization of the effective action for given vortex magnetic flux; similar considerations were already carried out in the framework of the Copenhagen vacuum [5]. Such more detailed approximations, e.g. an evaluation of the one-loop corrections, are deferred to future work.

It should however be emphasized that, though the explicit form of the coefficients of the various terms in the effective vortex action certainly depends on the approximation involved, the general structure of the gradient expansion of the vortex effective action is uniquely determined by Poincaré, gauge, and reparametrization invariance. In a forthcoming paper, the authors will use an action reminiscent of (111) with adjustable coefficients as a starting point for a phenomenological vortex model of infrared Yang-Mills physics.

5 Topology of Center Vortices

In the previous section, a rough sketch of a reduction of Yang-Mills theory to an effective vortex theory was given, by implementing a continuum version of the maximal center gauge, and by subsequently integrating out the Yang-Mills fields. Center-projected (or, more appropriately, vortex-projected) observables can in principle now be evaluated directly in terms of the vortex theory, which contains exclusively $(D-2)$ -dimensional vortex surface degrees of freedom in D -dimensional space-time.

There is an essential difference between the center vortices on the lattice and in the continuum theory. After center projection on the lattice, the direction of the magnetic flux of the vortex is lost, while in the continuum theory, the center vortices are given by oriented (patches of) surfaces, where the flux direction is defined by the orientation. This was already discussed to some extent in section 3.5.3. The orientation of the vortices, however, is crucial for their topological properties, as will be shown below by evaluating the Pontryagin index

$$\nu[A] = \frac{1}{32\pi^2} \int d^4x \tilde{F}_{\mu\nu}^a F_{\mu\nu}^a = -\frac{1}{16\pi^2} \int d^4x \text{tr} \tilde{F}_{\mu\nu} F_{\mu\nu} \quad (114)$$

using the ideal vortex representation (33).

It should be emphasized that the treatment in this section, the goal of which is to define the vortex-projected Pontryagin index, in some ways reverses the logic of the past sections. Whereas the continuum maximal center gauge and

also the vortex action were defined via the corresponding lattice expressions in the limit of vanishing lattice spacing, the Pontryagin index calls for a different treatment. It is initially defined for smooth continuum gauge field configurations, and useful lattice discretizations of the Pontryagin index are notoriously cumbersome. In fact, the maximal center gauge exacerbates the problem, since all lattice definitions at some point must assume the links of a lattice configuration to be reasonably close to unity. On the other hand, the maximal center gauge precisely transforms configurations into a form where their links strongly deviate from unity; namely, it introduces ideal vortices even into initially smooth configurations. Therefore, to properly define the vortex-projected Pontryagin index, it is necessary to start from the continuum expression, understanding the Pontryagin index for thin (or, gauge-equivalently, ideal) vortices to correspond to the thin limit of the Pontryagin index of thickened vortices, for which it is well-defined. This limit is smooth, as is demonstrated in an example in Appendix C; namely, the thick vortex profile function manifestly cancels. Note that this concept of vortex projection is not directly connected with lattice center projection anymore, since it is based on the thin limit of thickened (i.e. coset) configurations. In the following, the Pontryagin index will be evaluated for (thickened) ideal vortex configurations. The aforementioned example in Appendix C on the other hand treats a particular configuration of explicitly thick vortices, containing also the limiting case of thin vortices.

The field strength of an ideal center vortex \mathcal{A} is given by

$$\mathcal{F}_{\mu\nu}(k, x, S = \partial\Sigma) = F_{\mu\nu}[\mathcal{A}] = \partial_\mu \mathcal{A}_\nu(k, \Sigma, x) - \partial_\nu \mathcal{A}_\mu(k, \Sigma, x) \quad (115)$$

Straightforward evaluation (see Appendix A.1) yields for the field strength¹⁵ on a vortex surface S

$$\mathcal{F}_{\mu\nu}(k, x, S) = E(k) \int_S d^2 \tilde{\sigma}_{\mu\nu} \delta^4(x - \bar{x}(\sigma)) . \quad (116)$$

One can decompose a general vortex configuration into components of different center flux labeled by the integer k , where $k = 1, \dots, N - 1$ for $SU(N)$ color,

$$S = \bigcup_k S_k , \quad \mathcal{F}_{\mu\nu}(x, S) = \sum_k \mathcal{F}_{\mu\nu}(x, S_k) ; \quad (117)$$

Inserting this, and eq. (116), into (114), one finds for the Pontryagin index

$$\nu[\mathcal{A}] = -\frac{1}{8\pi^2} \sum_{k,k'} I(S_k, S_{k'}) \text{tr}(E(k)E(k')) \quad (118)$$

¹⁵In the context of superfluid Helium, this quantity is referred to as the vorticity tensor.

where

$$I(S_1, S_2) = \frac{1}{2} \int_{S_1} d^2 \tilde{\sigma}_{\mu\nu} \int_{S_2} d^2 \sigma'_{\mu\nu} \delta^4(\bar{x}(\sigma) - \bar{x}(\sigma')) \quad (119)$$

is the (oriented) intersection number between two two-dimensional surfaces S_1, S_2 in $D = 4$ space-time dimensions. Note that the intersection number $I(S_1, S_2)$ is also defined for open surfaces S_1, S_2 , and that, in $D = 4$ dimensions, $I(S_1, S_2) = I(S_2, S_1)$. Also, if S_1 and S_2 intersect in a single point, then $I(S_1, S_2) = \pm 1$, where the sign depends on the relative orientation of S_1 and S_2 . Note furthermore that, in the case $k = k'$ in (118), $I(S_k, S_k)$ counts each isolated self-intersection point of S_k twice. This is easily seen by further decomposing S_k into two components S_k^1 and S_k^2 such that neither of the two components self-intersect at the point in question. Then,

$$I(S_k, S_k) = I(S_k^1, S_k^1) + I(S_k^2, S_k^2) + 2I(S_k^1, S_k^2) \quad (120)$$

where the final term represents the contribution from the self-intersection point of S_k under consideration.

It should be remarked that this discussion of the self-intersection number $I(S, S)$ includes only the contributions from transversal intersection points, i.e. points where $\bar{x}_\mu(\sigma) = \bar{x}_\mu(\sigma')$ with $\sigma \neq \sigma'$, but leaves out the contribution from the coincidence points $\bar{x}_\mu(\sigma) = \bar{x}_\mu(\sigma')$ with $\sigma = \sigma'$. A more thorough discussion of the self-intersection number $I(S, S)$, which is given in Appendix B, does, however, not alter the conclusions on the Pontryagin index reached here.

Thus, the Pontryagin index of a vortex surface configuration is built up from its self-intersection points, each of which enters with a contribution $\pm 2 \cdot \text{tr}(E(k)E(k'))/8\pi^2$ into the Pontryagin index according to (118). The integers k, k' label the center flux carried by the two patches of the vortex surface configuration intersecting at the point in question; the sign depends on the relative orientation of the patches. In view of eq. (38), this implies specifically for $SU(2)$ color a contribution $\pm 1/2$ from each self-intersection point; on the other hand, for $SU(3)$ color, each self-intersection point contributes $\pm 1/3$ or $\pm 2/3$ to the Pontryagin index, cf. eqs. (41) and (42). This is consistent with the dependence on the number of colors noted by J. M. Cornwall in [29].

In view of this result, the reader might worry at this point about the integer-valuedness of the Pontryagin index on R^4 (silently compactified to S^4). This property cannot go lost during vortex projection, for the very simple reason that vortices can be explicitly represented as gauge field configurations and

therefore inherit all properties known to be true for generic gauge fields. Nevertheless, it is instructive to remark how the integer-valuedness comes about in more detail in a simple case, namely $SU(2)$ vortices on R^4 . It is due to the fact well-known in topology¹⁶ that the number of intersection points of two closed two-dimensional surfaces in R^4 is even. This also implies that the number of self-intersection points of a closed surface is even, because the self-intersection number is defined by simply intersecting the surface with another surface infinitesimally displaced from it (i.e. one considers a framing of the surface, cf. Appendix B). Thus, while each self-intersection point of an $SU(2)$ vortex surface configuration gives a contribution $\pm 1/2$ to the Pontryagin index, the number of such contributions is even, and the Pontryagin index integer-valued.

In the case of higher $SU(N)$ gauge groups, the argument becomes more complicated, since the surfaces may branch and also due to the fact that superimposed Dirac strings in general also modify the type of vortex flux, i.e. its direction in color space. Further complications arise on different space-time manifolds. For instance, on a four-cube with periodic boundary conditions, i.e. a torus, one might think of generating a single intersection point between two surfaces by choosing e.g. the 1-2 plane and the 3-4 plane, which are closed due to the periodic boundary conditions. However, this example is invalid, since vortex surfaces must be representable as surfaces of three-volumes, which is not the case for the aforementioned planes.

The final point to be discussed is the fact, also well-known in topology, that the self-intersection number of closed, *globally oriented* two-dimensional surfaces in R^4 not only is a multiple of four (remember that each intersection point is counted doubly, and there are an even number of intersection points for closed surfaces), but actually vanishes. This implies that the Pontryagin index vanishes for globally oriented vortex surfaces; conversely, therefore, non-orientedness of the surfaces is crucial for generating a non-vanishing topological winding number. To illustrate this, consider the following three-dimensional slice of two intersecting $SU(2)$ vortex surfaces in $D = 4$ dimensions, cf. Fig. 3. Let the one vortex be located entirely within the three-dimensional slice of space-time under consideration; it is therefore visible as a closed surface, namely the sphere S in Fig. 3. On the other hand, let the other vortex extend into the space-time dimension not displayed in Fig. 3; it is then visible as a closed loop C after slicing. Let C intersect S at two

¹⁶The authors thank B. Leeb for a discussion on this point.

points, chosen in Fig. 3 as the poles of S .

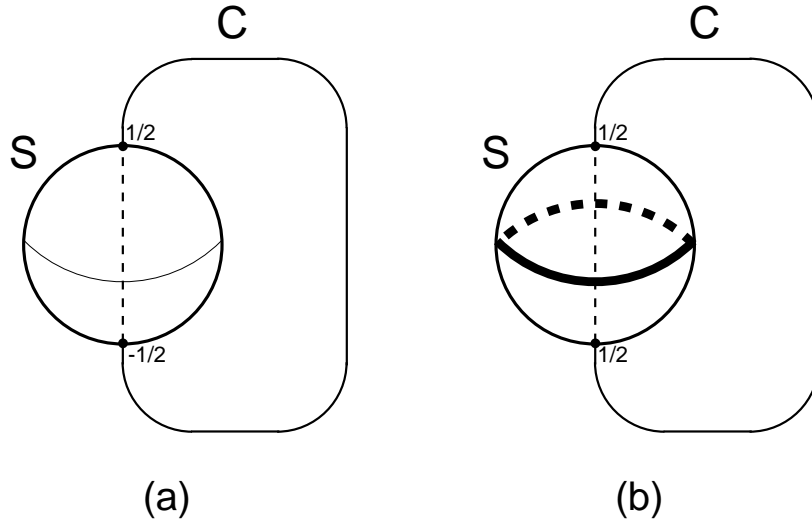


Figure 3: Three-dimensional slice of two intersecting $SU(2)$ vortex surfaces in four space-time dimensions (see text). The thin line around the equator of the sphere S in (a) is merely to guide the eye in identifying S as a sphere. At the intersection points of S and C , contributions to the Pontryagin index of modulus $1/2$ arise. However, in the case of globally oriented surfaces (a), these contributions cancel. On the other hand, in the case that vortex surfaces are not globally oriented, but consist of patches of different orientation (b), the contributions may add, giving rise to a nonvanishing Pontryagin index. Boundaries of such patches are tagged by Abelian monopoles (thick line around the equator in (b)).

If S and C are both globally oriented, as in Fig. 3 (a), their intersection number (in $D = 3$)

$$I(S, C) = \int_S d^2\tilde{\sigma}_i \int_C dx_i \delta^3(x - \bar{x}(\sigma)) \quad (121)$$

vanishes, since the two intersection points occur with opposite relative orientation between the intersecting manifolds. Thus, a non-zero intersection number requires at least one of the two intersecting closed manifolds to be not globally oriented. Globally non-oriented hypersurfaces consist nevertheless of oriented patches. Assume for example the sphere S in Fig. 3 (b) to

consist of two hemispheres of opposite orientation. E.g., the southern hemisphere may be covered by a Dirac string world-sheet, simply reversing (in the case of $SU(2)$ color) the orientation associated with that hemisphere. The boundary of a Dirac string world-sheet is complemented by a monopole in the Abelian-projected configuration, cf. eq. (103). Thus, in Fig. 3 (b), one can associate an Abelian monopole current with the equator (thick line). Further below, it will be shown more generally how boundaries of oriented patches on vortex surfaces imply monopole currents.

Now, in the presence of the monopole current at the equator in Fig. 3 (b), implying a reversal in orientation of, say, the southern hemisphere, the contributions to the Pontryagin index from the two intersection points no longer cancel, but add coherently, giving a Pontryagin index of modulus $|\nu| = 1$. Thus, the depicted configuration represents an analogue of an instanton in the sense that it will generate a zero mode in the Dirac operator according to the index theorem. The authors speculate that standard smoothing procedures used on the lattice to detect instantons would transmute this configuration into an instanton, since smoothing by construction alters configurations such as to lower the Yang-Mills action. After smoothing, it is impossible to discern what type of excitation precisely carried Pontryagin index in the original configuration. Note that this picture of the generation of topological winding number also correlates well with the observation [33],[34] that instantons are encircled by monopole loops in the maximal Abelian gauge. It is precisely the monopole loop which tags the change in orientation in the vortex surface (the sphere S in Fig. 3 (b)) between the two intersection points carrying the topological density, causing their contributions to the Pontryagin index to add up and generate the “pre-instanton”.

To see the emergence of the magnetic monopole loops at the boundaries of vortex surface patches in more detail, consider an isolated patch; this now represents an open two-dimensional surface sheet S with boundary $\partial S = C$. To this surface S , one can relate a magnetic flux sheet by associating with it the field strength (see above)

$$\mathcal{F}_{\mu\nu}(x, S) = E \int_S d^2\tilde{\sigma}_{\mu\nu} \delta^4(x - \bar{x}(\sigma)) . \quad (122)$$

For a closed surface $S = \partial\Sigma$, this expression agrees with the one for the ideal vortex $\mathcal{A}(\Sigma, x)$ given in (116). By Stokes’ theorem, one finds that a conserved (Abelian) magnetic current

$$j_\mu^m(x, C) = \partial_\nu \tilde{\mathcal{F}}_{\mu\nu} = E \oint_{\partial S=C} dy_\mu \delta^4(x - y) , \quad \partial_\mu j_\mu^m(x, C) = 0 \quad (123)$$

must flow at the boundary $\partial S = C$ of the magnetic sheet S . Note that the direction of the magnetic current on $\partial S = C$ defines an orientation of the sheet S and vice versa. This monopole current is generated by a magnetic point charge q^m

$$Eq^m = \int_V d\tilde{\sigma}_\mu j_\mu^m(x, C) = EI(V, C) \quad (124)$$

with V denoting the three-volume dual to the loop C . In view of $\exp(-E) = Z$, eq. (124) yields for q^m only a fraction of the elementary magnetic charge dictated by the Dirac quantization condition. This is as it should be, since the vortex sheet S only carries a fraction of the flux which a Dirac string carries. Only when glueing the open vortex patches with their boundary monopole loops back together, should one take care to obtain current loops of proper magnetic point charges satisfying the Dirac quantization condition. In this way, non-oriented closed magnetic vortex sheets are constructed, consisting of oriented surface pieces joined by magnetic monopole current loops¹⁷. Such a non-oriented closed magnetic sheet defines a center vortex which still gives the same contribution to a Wilson loop as the corresponding oriented vortex (in the absence of a monopole loop), cf. eq. (43). Thus, for the confinement properties, measured by the Wilson loop, the orientation of a vortex sheet, and hence the magnetic monopole currents, are irrelevant. The Abelian magnetic monopole currents are however necessary in order to generate a non-vanishing Pontryagin index for vortex configurations. It is in fact easy to see that the Pontryagin index of the vortices can be determined from the Abelian magnetic monopoles alone. Indeed, inserting (115) into (114), after a partial integration the Pontryagin index of an ideal vortex sheet becomes

$$\nu = -\frac{1}{8\pi^2} \int_{\mathcal{M}} \partial_\mu \text{tr} (\mathcal{A}_\nu \tilde{\mathcal{F}}_{\mu\nu}) + \frac{1}{8\pi^2} \int_{\mathcal{M}} \text{tr} \mathcal{A}_\nu \partial_\mu \tilde{\mathcal{F}}_{\mu\nu} \quad (125)$$

$$= -\frac{1}{8\pi^2} \int_{\partial\mathcal{M}} d\sigma_\mu \text{tr} (\mathcal{A}_\nu \tilde{\mathcal{F}}_{\mu\nu}) + \frac{1}{8\pi^2} \int_{\mathcal{M}} \text{tr} \mathcal{A}_\nu j_\nu^m(x, C) \quad (126)$$

where Gauß' law was used in the first term and the definition of the magnetic current in the second term. The second term obviously vanishes in the absence of magnetic monopoles. Furthermore, the surface term vanishes unless the integrand contains singularities which give rise to internal surfaces wrapping the singularities. Such internal surfaces precisely arise in the presence of magnetic charges [14] which may be magnetic monopoles or

¹⁷If one glues together two patches such that the surface orientation does not change across the boundary, the monopole currents at the boundary precisely cancel.

more extended magnetic charge distributions such as line or surface charges. Thus, a non-zero Pontryagin index requires the existence of magnetic charges in Abelian-projected configurations. This is consistent with the findings in [14].

6 Outlook

In this work, the continuum analogues of the maximal center gauge and center projection in lattice Yang-Mills theory were constructed. This shed new light on the meaning of the procedure on the lattice and led to a sketch of an effective vortex theory in the continuum. Also the manner in which center vortex configurations generate the Pontryagin index was clarified; the latter is built up from self-intersections of the vortex network, where it is crucial that the vortex surfaces be globally non-oriented. Since these developments have already been discussed at length in the corresponding sections above, it suffices here to mention some open issues which require further investigation.

With regard to the maximal center gauge, it is necessary to conduct lattice experiments using alternative gauge fixing functions \bar{g} , cf. eq. (6), and to test whether the physical conclusions reached using the direct maximal center gauge remain unaffected. If it is true that maximal center gauges provide a rough localization of thick vortices present in full lattice configurations, then long-distance properties should be robust with respect to a variation of \bar{g} ; fluctuations of the center projection vortices within the thick vortex profile are of course gauge-dependent, as evidenced in section 2.2. An issue which is of particular interest in this context is the occurrence of Gribov copies which do not correspond to the absolute maximum of the center gauge fixing functional. In [19], the possibility is raised that the true gauge fixing image selected in particular by the direct maximal center gauge contains less vortices than found in previous studies, and no vortex confinement. As discussed in sections 3.5.1 and 3.5.2, the direct maximal center gauge in the continuum limit in fact always selects a trivial gauge fixing image devoid of center vortices. The observations of [19] may be a signature of the specific problems of this particular gauge. On the other hand, it is straightforward to formulate alternative gauge fixing functions \bar{g} which prevent these problems. It would be interesting to repeat the considerations of [19] using such a gauge.

Concerning the issue of an effective vortex theory, it was already mentioned in section 4 that the authors plan to report on their numerical study of a phenomenological random surface model for vortices in a forthcoming paper. On the other hand, from an analytical point of view, it would presumably be helpful to start with lower-dimensional models. E.g., it would be worthwhile to study whether the maximal center gauge allows a solution of Yang-Mills theory in $1+1$ space-time dimensions; there, the effective vortex theory takes the form of a classical statistical mechanics of vortex points.

Finally, it is necessary to investigate whether center vortices do in fact fully capture the physics of the Pontryagin index; i.e. one should test whether the vortex-projected Pontryagin index displays vortex dominance in analogy to the center dominance observed for the string tension. While it has been shown in this work how vortices generate a nontrivial topological winding number, and the converse experiment in [16] has shown that an ensemble devoid of center vortices is concentrated in the trivial topological sector, the question of vortex dominance is more stringent. In this context, it is worth mentioning the analogous result from Abelian-projected theories: In the maximal Abelian gauge, one finds monopole dominance in the string tension [9], but not in the Pontryagin index; on the other hand, in the Polyakov gauge, the monopole dominance in the string tension is much less pronounced, but the Pontryagin index can be reconstructed exactly from the monopole content of the gauge-fixed configurations alone [14].

In connection with the issue of the Pontryagin index, of course also a more detailed study of chiral symmetry breaking by a vortex background is called for. Vortex configurations which give rise to a non-vanishing Pontryagin index must, by the index theorem, give rise to zero modes of the Dirac operator. It would e.g. be interesting to explicitly construct such zero modes for some relevant simple vortex configurations. In the context of instanton models, the zero modes induced by the instantons give in fact the dominant contribution to the chiral condensate. The question arises whether the chiral condensate displays vortex dominance (again, the converse experiment [16] yields zero condensate in the absence of vortices), and, if so, how it behaves at finite temperatures, in particular, at the deconfinement transition.

Acknowledgements

Discussions with K. Langfeld and B. Leeb are gratefully acknowledged.

A Properties of center vortices

A.1 The ideal center vortex

In the following, the field strength $F_{\mu\nu}[\mathcal{A}]$ of the ideal vortex field $\mathcal{A}(k, \Sigma, x)$ is calculated. For this purpose, it is convenient to evaluate first its dual,

$$\tilde{\mathcal{F}}_{\mu\nu} = \frac{1}{2}\epsilon_{\mu\nu\alpha\beta}F_{\alpha\beta}[\mathcal{A}] = \epsilon_{\mu\nu\alpha\beta}\partial_\alpha\mathcal{A}_\beta(k, \Sigma, x) \quad (127)$$

Inserting here the explicit representation for $\mathcal{A}_\beta(k, \Sigma, x)$, cf. eq. (33), one obtains

$$\tilde{\mathcal{F}}_{\mu\nu}(k, \partial\Sigma, x) = E(k)\epsilon_{\mu\nu\kappa\lambda}\int_\Sigma d^{D-1}\tilde{\sigma}_\lambda\partial_\kappa^x\delta^D(x - \bar{x}(\sigma)) \quad (128)$$

$$= E(k)\frac{1}{3!}\epsilon_{\mu\nu\kappa\lambda}\epsilon_{\lambda\alpha\rho\gamma}\int d^{D-1}\sigma_{\alpha\rho\gamma}\partial_\kappa^x\delta^D(x - \bar{x}(\sigma)) \quad (129)$$

$$= E(k)\int_\Sigma d^{D-1}\sigma_{\kappa\mu\nu}\partial_\kappa^{\bar{x}}\delta^D(x - \bar{x}(\sigma)) \quad (130)$$

Application of Stokes' theorem yields

$$\tilde{\mathcal{F}}_{\mu\nu}(k, \partial\Sigma, x) = E(k)\int_{\partial\Sigma} d^{D-2}\sigma_{\mu\nu}\delta^D(x - \bar{x}(\sigma)) . \quad (131)$$

Taking the dual of this equation yields the desired representation (116).

With the vortex field strength eq. (131) the Yang-Mills action of an ideal vortex in $D = 4$ space-time dimensions is given (up to an unimportant numerical factor) by

$$\bar{S} = \int_{\partial\Sigma} d^2\sigma_{\mu\nu}\int_{\partial\Sigma} d^2\sigma'_{\mu\nu}\delta^4(\bar{x}(\sigma) - \bar{x}(\sigma')) . \quad (132)$$

Obviously this action is divergent and calls for regularization. Regularization will be achieved by chopping off the high frequencies using an ultraviolet cutoff Λ ; this amounts to replacing the δ -function in equation (132) by the regularized version

$$\delta(x) = \frac{\Lambda}{\sqrt{2\pi}}e^{-\frac{\Lambda^2}{2}x^2} . \quad (133)$$

Before proceeding, a comment is in order concerning the thin limit $\Lambda \rightarrow \infty$. As long as Λ is arbitrarily large, but fixed with respect to the ultraviolet regulator of the theory, say the inverse lattice spacing, it is legitimate to evaluate the action using the continuum Yang-Mills expression (132). However, if the vortex is meant to be truly thin, i.e. if its entire magnetic flux is

concentrated on one lattice plaquette, then one must use the lattice plaquette expression for the action; otherwise, one loses track of the compact character of the gauge group. E.g., if one exactly superimposes two truly thin $SU(2)$ ideal vortices on top of each other (this corresponds to a closed Dirac string), then naive application of the continuum Yang-Mills expression for the action would lead to a value diverging like four times the action of a single vortex. On the other hand, all plaquettes encircling this Dirac string take the value (+1), and its action therefore vanishes, as it should¹⁸.

Keeping this caveat in mind, the regularized action can be evaluated in a gradient expansion. Note that similar calculations have been performed in [35],[36] for a massive propagator. Since the action receives contributions only from $\bar{x}(\sigma) \simeq \bar{x}(\sigma')$, the integrand (132) can be expanded in powers of $z = \sigma - \sigma'$. Defining $s = \frac{\sigma + \sigma'}{2}$ and expanding (where $\partial_a = \partial/\partial\sigma_a$),

$$\begin{aligned}\bar{x}(\sigma) &= \bar{x}(s) + \frac{z^a}{2} \partial_a \bar{x}(s) + \dots \\ \bar{x}(\sigma') &= \bar{x}(s) - \frac{z^a}{2} \partial_a \bar{x}(s) \\ \Sigma_{\mu\nu}(\sigma) &= \Sigma_{\mu\nu}(s) + \frac{z^a}{2} \partial_a \Sigma_{\mu\nu}(s) + \frac{1}{2} \frac{z^a}{2} \frac{z^b}{2} \partial_a \partial_b \Sigma_{\mu\nu}(s) + \dots \\ \Sigma_{\mu\nu}(\sigma') &= \Sigma_{\mu\nu}(s) - \frac{z^a}{2} \partial_a \Sigma_{\mu\nu}(s) + \frac{1}{2} \frac{z^a}{2} \frac{z^b}{2} \partial_a \partial_b \Sigma_{\mu\nu}(s) + \dots, \quad (134)\end{aligned}$$

one obtains

$$\begin{aligned}\bar{S} &= \left(\frac{\Lambda}{\sqrt{4\pi}} \right)^4 \int_{\partial\Sigma} d^2\sigma \int_{-\infty}^{\infty} d^2z e^{-\frac{\Lambda^2}{2} z^a g_{ab}(\sigma) z^b} \left[(\Sigma_{\mu\nu}(\sigma))^2 \right. \\ &\quad \left. - \frac{z^a}{2} \frac{z^b}{2} \partial_a \Sigma_{\mu\nu}(\sigma) \partial_b \Sigma_{\mu\nu}(\sigma) + \frac{z^a}{2} \frac{z^b}{2} \Sigma_{\mu\nu}(\sigma) \partial_a \partial_b \Sigma_{\mu\nu}(\sigma) \right], \quad (135)\end{aligned}$$

where only terms up to order z^2 in both the exponent and preexponent have been kept. Furthermore, the range of integration over z has been extended to $\pm\infty$, since the main contribution to the integral comes from the region $z \approx 0$. Carrying out the Gaussian integration over z , one obtains

$$\bar{S} = \left(\frac{\Lambda}{\sqrt{2\pi}} \right)^2 \int_{\partial\Sigma} d^2\sigma \left[2\sqrt{g} + \frac{1}{\Lambda^2} \left(\partial_a \Sigma_{\mu\nu} \partial_b \Sigma_{\mu\nu} - \frac{1}{2} \partial_a \partial_b g \right) \frac{\partial}{\partial g_{ab}} \frac{1}{\sqrt{g}} \right]. \quad (136)$$

¹⁸In the case of the Dirac string, these subtleties can be circumvented by dividing the space-time manifold into coordinate patches as in the Wu-Yang construction.

Here, the metric on the vortex sheet has been introduced,

$$g_{ab}(\sigma) = \partial_a \bar{x}_\mu(\sigma) \partial_b \bar{x}_\mu(\sigma), \quad g = \det(g_{ab}). \quad (137)$$

Furthermore, a partial integration has been performed in the last term of equation (135). The expression obtained above can be cast into a more standard form by using the decomposition

$$\partial_a \partial_b \bar{x}_\mu(\sigma) = \Gamma_{ab}^c \partial_c \bar{x}_\mu + K_{ab}^A n_\mu^A, \quad (138)$$

where Γ_{ab}^c are the affine connections and K_{ab}^A denotes the extrinsic curvature. Furthermore, n_μ^A , with $A = 1, 2$, are unit vectors orthogonal to the tangent vector of the vortex sheet

$$n_\mu^A \partial_c \bar{x}_\mu(\sigma) = 0, \quad n_\mu^A n_\mu^B = \delta^{AB}, \quad A = 1, 2. \quad (139)$$

Using

$$\epsilon^{ab} g_{bd} \epsilon^{cd} = g^{ac} \cdot g \quad (140)$$

one eventually obtains after straightforward evaluation

$$\bar{S} = \left(\frac{\Lambda}{\sqrt{2\pi}} \right)^2 \int_{\partial\Sigma} d^2\sigma \sqrt{g} \left[2 - \frac{1}{\Lambda^2} g^{ab} g^{ik} K_{ai}^A K_{bk}^A + \frac{\sqrt{g}}{2\Lambda^2} g^{ab} \partial_a \partial_b \ln \sqrt{g} \right]. \quad (141)$$

The first term, which diverges for $\Lambda \rightarrow \infty$, is the familiar Nambu-Goto term. The remaining two terms are finite for $\Lambda \rightarrow \infty$. The second term, containing the extrinsic curvature coefficients K_{ai}^a , has been discussed in [31],[32]. The higher-order terms in the gradient expansion all vanish for $\Lambda \rightarrow \infty$.

A.2 The thin center vortex

In the following, it is shown that the thin center vortex as defined by eq. (62) for arbitrary vortex shapes $S = \partial\Sigma$ indeed yields a center element for the Wilson loop when non-trivially linked to it. For this purpose, it is convenient to write the thin vortex as

$$a_\mu(k, S, x) = E(k) \alpha_\mu(S, x) \quad (142)$$

$$\alpha_\mu(S, x) = \int_S d^{D-2} \tilde{\sigma}_{\mu\kappa} \partial_\kappa^x D(x - \bar{x}(\sigma)) \quad (143)$$

Using Stokes' theorem, one obtains

$$\oint_C dx_\mu \alpha_\mu(S, x) = \int_{M(C)} d^2 \sigma_{\lambda\mu} \partial_\lambda^x \alpha_\mu(S, x) \quad (144)$$

$$= \int_{M(C)} d^2 \sigma_{\lambda\mu} \int_S d^{D-2} \tilde{\sigma}_{\mu\kappa} \partial_\lambda^x \partial_\kappa^x D(x - \bar{x}(\sigma)) \quad (145)$$

where $C = \partial M$. By using the relation between $d\sigma_{\mu\nu}$ and its dual $d\tilde{\sigma}_{\mu\nu}$, the last expression can be rewritten as

$$\oint_C dx_\mu \alpha_\mu(S, x) = -\frac{1}{4} \int_{M(C)} d^2 \tilde{\sigma}_{\alpha'\beta'} \int_S d^{D-2} \tilde{\sigma}_{\alpha\beta} \epsilon_{\mu\nu\alpha'\beta'} \epsilon_{\mu\kappa\alpha\beta} \partial_\lambda^x \partial_\kappa^x D(x - \bar{x}(\sigma)) \quad (146)$$

Using the properties of $\epsilon_{\alpha\beta\gamma\delta}$, this expression can be converted to

$$\begin{aligned} \oint_C dx_\mu \alpha_\mu(S, x) &= -\frac{1}{2} \int_{M(C)} d^{D-2} \tilde{\sigma}_{\alpha\beta}(x) \int_S d^2 \sigma_{\alpha\beta}(\bar{x}) \partial_x^2 D(x - \bar{x}) \quad (147) \\ &\quad + \int_{M(C)} d^{D-2} \tilde{\sigma}_{\kappa\beta} \int_S d^2 \sigma_{\alpha\beta} \partial_\alpha \partial_\kappa D(x - \bar{x}) \quad (148) \end{aligned}$$

The last term is seen to vanish by Stokes' theorem, since $\partial S = \partial(\partial\Sigma) = 0$. The first term yields, upon using the definition of the Green's function, the intersection number between $M(C)$ and S ,

$$\oint_C dx_\mu \alpha_\mu(S, x) = \frac{1}{2} \int_{M(C)} d^{D-2} \tilde{\sigma}_{\alpha\beta}(x) \int_S d^2 \sigma_{\alpha\beta}(\bar{x}) \delta^D(x - \bar{x}) \quad (149)$$

$$= I(M(C), S) \quad (150)$$

$$= L(C, S) \quad (151)$$

which equals the linking number between C and S , i.e. $L(C, S)$. With the last relation, one indeed obtains a center element for the Wilson loop from the thin vortex (62),

$$\exp\left(-\oint_C dx_\mu a_\mu(k, S, x)\right) = \exp(-E(k)L(C, S)) = Z(k)^{L(C, S)} \quad (152)$$

B Intersection number of two-dimensional sheets in $D = 4$

This appendix summarizes essential properties of the self-intersection number of two-dimensional surfaces in $D = 4$ space-time dimensions; in particular,

the relation of the self-intersection number to topological invariants of the three-dimensional spaces located at the initial and final times is presented. Assume a certain parametrization of the vortex sheet $\bar{x}_\mu(\sigma) \equiv \bar{x}_\mu(\sigma_1, \sigma_2)$ in $D = 4$. The self-intersection number $I(S, S)$, cf. eq. (119), i.e., the intersection number of S with itself, receives contributions from “coincidence points” $\bar{x}_\mu(\sigma) = \bar{x}_\mu(\sigma')$ with $\sigma = \sigma'$ and from (transversal) “intersection points” $\bar{x}_\mu(\sigma) = \bar{x}_\mu(\sigma')$ with $\sigma \neq \sigma'$, which will be denoted by $I_1(S, S)$ and $I_2(S, S)$ respectively,

$$I(S, S) = I_1(S, S) + I_2(S, S) \quad (153)$$

Regularizing the delta function in eq. (119), cf. Appendix A.1, eq. (133), introduces an ultraviolet cutoff Λ , which then allows $I_1(S, S)$ to be straightforwardly evaluated; in the limit $\Lambda \rightarrow \infty$, one finds Polyakov’s intersection number¹⁹,

$$I_1(S, S) = -\frac{1}{16\pi} \int_S \frac{d^2\sigma}{\sqrt{g}} g^{ij} \partial_i \Sigma_{\mu\nu} \partial_j \tilde{\Sigma}_{\mu\nu} \quad (154)$$

where

$$g_{ij} = \partial_i \bar{x}_\mu(\sigma) \partial_j \bar{x}_\mu(\sigma) \quad (155)$$

denotes the metric on the surface S , $g = \det g_{ij}$ and

$$\Sigma_{\mu\nu} = \epsilon_{ij} \partial_i \bar{x}_\mu(\sigma) \partial_j \bar{x}_\nu(\sigma) \quad (156)$$

is the tensor of the surface element on the vortex sheet.

Let $\bar{x}_\mu(\sigma(k)) = \bar{x}_\mu(\sigma'(k))$, where $\sigma(k) \neq \sigma'(k)$, determine the coordinates of isolated (self-)intersection points $P(k)$ of S . Expanding $\bar{x}_\mu(\sigma), \bar{x}_\mu(\sigma')$ near $\sigma = \sigma(k), \sigma' = \sigma'(k)$ in powers of $\sigma - \sigma(k), \sigma' - \sigma'(k)$, the integrals in (119) over $d^2\sigma, d^2\sigma'$ can be straightforwardly performed, yielding

$$I_2(S, S) = 2 \sum_k \text{sign} \left(\Sigma_{\mu\nu}(\bar{x}(\sigma(k))) \tilde{\Sigma}_{\mu\nu}(\bar{x}(\sigma(k))) \right) \quad (157)$$

One observes that each intersection point $\bar{x}_\mu(\sigma(k)) = \bar{x}_\mu(\sigma'(k))$, with $\sigma(k) \neq \sigma'(k)$, contributes doubly to the self-intersection number $I_2(S, S)$ in agreement with the findings in section 5.

¹⁹ $I_1(S, S)$ differs from Polyakov’s original definition [31] by a factor of $(-\frac{1}{4})$.

To illustrate the geometric meaning of the different contributions to the intersection number, it is useful to consider a fixed time slice of the four-dimensional universe. In this three-dimensional space, the vortex S represents a closed loop $C(t = \text{fixed})$. For simplicity, choose $t = \sigma_2$ such that this loop is parametrized by σ_1 , which takes values in $[0, 2\pi[$.

Consider the self-linking number $SL(C, \hat{n})$ of such a closed loop $C(t)$ in $D = 3$, which is defined by the linking number $L(C, C')$ between the original loop $C(t)$ and the fictitious loop $C'(t)$ resulting from $C(t)$ by an infinitesimal shift

$$\bar{x}_\mu(\sigma_1, t) \rightarrow \bar{x}_\mu(\sigma_1, t) + \epsilon \hat{n}(\sigma_1, t) . \quad (158)$$

Here, $\hat{n}(\sigma_1, t)$ is a unit vector perpendicular to the tangent vector $\vec{x}'(\sigma_1, t) = \frac{\partial}{\partial \sigma_1} \vec{x}(\sigma_1, t)$ of the loop $C(t)$,

$$\hat{n}(\sigma_1, t) \cdot \vec{x}'(\sigma_1, t) = 0, \quad \hat{n}^2 = 1 \quad (159)$$

which is periodic in σ_1 , $\hat{n}(\sigma_1 + 2\pi, t) = \hat{n}(\sigma_1)$, i.e.

$$SL(C, \hat{n}) = \lim_{\epsilon \rightarrow 0} L(C, C') . \quad (160)$$

In this last equation,

$$L(C, C') = \frac{1}{4\pi} \oint_C \oint_{C'} d\vec{x} \times d\vec{x}' \frac{\vec{x} - \vec{x}'}{|\vec{x} - \vec{x}'|} \quad (161)$$

is the familiar Gauß linking number.

The vector $\hat{n}(\sigma_1, t)$ defines a framing of the loop $C(t)$, which implies a thickening of the loop into a ribbon bounded by $C(t)$ and $C'(t)$. Let \bar{C} denote the loop along the middle of this ribbon which is generated by $\vec{x}(\sigma_1, t) + \frac{\epsilon}{2} \hat{n}(\sigma_1, t)$ with t fixed. Taking the limit $\epsilon \rightarrow 0$, one finds for the self-linking number [37]

$$SL(C, \hat{n}) = W_r(C) + T_w(C, \hat{n}) \quad (162)$$

Here

$$W_r(C) = L(\bar{C}, \bar{C}) \quad (163)$$

is the writhing number and

$$T_w(C, \hat{n}) = \frac{1}{2\pi} \oint d\sigma_1 [\vec{e}(\sigma_1, t) \times \hat{n}(\sigma_1, t)] \cdot \hat{n}'(\sigma_1, t) \quad (164)$$

denotes the twist, where

$$\vec{e}(\sigma_1, t) = \frac{\vec{x}'(\sigma_1, t)}{|\vec{x}'(\sigma_1, t)|} \quad (165)$$

is the unit vector tangential to the loop $C(t)$. The twist $T_w(C, \hat{n})$ is not a topological invariant but depends on the choice of the framing $\hat{n}(\sigma_1, t)$. A global change of $\hat{n}(\sigma_1, t)$ changes $T_w(C, \hat{n})$ by some integer. The twist $T_w(C, \hat{n})$ expresses the torsion of the ribbon bounded by $C(t)$ and $C'(t)$ and represents the Polyakov spin factor in $D = 3$. It should be emphasized that, while the self-linking number and the twist depend on the choice of the framing $\hat{n}(\sigma_1, t)$, their difference, i.e. the writhing number, is independent of this arbitrariness. Furthermore, it can be shown that the self-intersection number $I_2(S, S)$ is related to the difference in the self-linking number between the initial and final time t_1 and t_2 of the four-dimensional space-time manifold [36]

$$I_2(S, S) = -SL(C(t), \hat{n}(t))\Big|_{t=t_1}^{t=t_2} . \quad (166)$$

In an analogous way, Polyakov's intersection number is related to the twist of $C(t)$,

$$I_1(S, S) = T_w(C(t), \hat{n}(t))\Big|_{t=t_1}^{t=t_2} , \quad (167)$$

so that the total intersection number is given by the writhing number

$$I(S, S) = -W_r(C(t))\Big|_{t=t_1}^{t=t_2} . \quad (168)$$

A transversal self-intersection point of the vortex sheet gives rise to a self-intersection point of the vortex string $C(t)$ at some time \bar{t} . If the loop $C(t)$ self-intersects at some time $t = \bar{t}$, the writhing number changes by 2 from the time before \bar{t} until the time after the intersection. This contribution 2 corresponds to the fact that each (transversal) self-intersection point of the vortex sheet contributes 2 units to the intersection number. Since for all closed vortex sheets, self-intersection points occur pairwise, the vortex string $C(t)$ must self-intersect an even number of times, so that the $SU(2)$ Pontryagin index

$$\nu[A(S)] = -\frac{1}{4}W_r(C(t))\Big|_{t=t_1}^{t=t_2} \quad (169)$$

becomes an integer, as observed already in section 5.

C Topological charge of a thick SU(2) vortex intersection

Consider two intersecting planar thick $SU(2)$ vortices in four space-time dimensions. By choice of coordinate system, the intersection region can be centered on the origin of space-time, and one of the vortices can be centered on the 1-2-plane,

$$A^{(1)} = T_3 \frac{f_1(x_3^2 + x_4^2)}{x_3^2 + x_4^2} (0, 0, x_4, -x_3) \quad (170)$$

cf. eq. (10), with an arbitrary profile function f_1 . On the other hand, let the other vortex be centered on the 3' - 4'-plane of a (primed) coordinate system related to the previous one by an arbitrary orthogonal transformation O ,

$$A^{(2)'} = T_3 \frac{f_2(x_1'^2 + x_2'^2)}{x_1'^2 + x_2'^2} (x_2', -x_1', 0, 0) \quad (171)$$

$$x'_i = O_{ij} x_j \quad (172)$$

This also defines the transformation of the direction of the four-vector $A^{(2)'}$ when going to the unprimed coordinate system, $A^{(2)} = O^T A^{(2)'}$. In the unprimed coordinate system, therefore, the second thick vortex is given by

$$A_i^{(2)} = T_3 \frac{f_2[(O_{1j}x_j)^2 + (O_{2k}x_k)^2]}{(O_{1l}x_l)^2 + (O_{2m}x_m)^2} (O_{1i}O_{2p}x_p - O_{2i}O_{1q}x_q) \quad (173)$$

From this, one straightforwardly obtains the field strengths associated with the thick vortex fields (where the prime on the profile functions denotes differentiation w.r.t. the argument),

$$F_{34}^{(1)} = -F_{43}^{(1)} = \partial_3 A_4^{(1)} - \partial_4 A_3^{(1)} = -2T_3 f_1'(x_3^2 + x_4^2) \quad (174)$$

$$F_{ij}^{(1)} = 0 \quad \text{otherwise} \quad (175)$$

and

$$F_{ij}^{(2)} = \partial_i A_j^{(2)} - \partial_j A_i^{(2)} \quad (176)$$

$$= 2T_3 (O_{1j}O_{2i} - O_{2j}O_{1i}) f_2' \left((O_{1k}x_k)^2 + (O_{2l}x_l)^2 \right). \quad (177)$$

The Pontryagin index is given by

$$\nu = -\frac{1}{32\pi^2} \int d^4x \epsilon_{ijkl} \text{tr}(F_{ij} F_{kl}) \quad (178)$$

One can easily verify that the integrand vanishes for each thick vortex taken separately,

$$\epsilon_{ijkl}\text{tr}(F_{ij}^{(1)}F_{kl}^{(1)}) = \epsilon_{ijkl}\text{tr}(F_{ij}^{(2)}F_{kl}^{(2)}) = 0 \quad (179)$$

and therefore the only nonvanishing contribution to ν results from the intersection region of the two thick vortices,

$$\begin{aligned} \nu &= -\frac{1}{4\pi^2} \int d^4x \text{tr}(F_{12}^{(2)}F_{34}^{(1)}) \\ &= -\frac{1}{2\pi^2} \int d^4x (O_{12}O_{21} - O_{22}O_{11}) f_2' \left((O_{1k}x_k)^2 + (O_{2l}x_l)^2 \right) f_1'(x_3^2 + x_4^2) \end{aligned} \quad (180)$$

By the change of integration variables

$$(x_1, x_2) \longrightarrow (x'_1, x'_2) = (O_{1k}x_k, O_{2l}x_l) \quad (181)$$

this simplifies (up to the sign of the Jacobian) to

$$|\nu| = \frac{1}{2\pi^2} \int dx'_1 dx'_2 dx_3 dx_4 f_2'(x_1'^2 + x_2'^2) f_1'(x_3^2 + x_4^2) \quad (182)$$

$$= 2 \int_0^\infty dr \int_0^\infty dr' r r' f_2'(r'^2) f_1'(r^2) \quad (183)$$

$$= \frac{1}{2} f_2(r'^2) \Big|_0^\infty \cdot f_1(r^2) \Big|_0^\infty \quad (184)$$

Due to the boundary conditions on profile functions (cf. the description after eq. (10)), one thus finally obtains

$$|\nu| = \frac{1}{2}, \quad (185)$$

generalizing the result for thin $SU(2)$ vortices derived in section 5. The specific form of the profile functions has completely canceled, and the present treatment thus in particular also includes the case of thin $SU(2)$ vortices. Also all reference to the coordinate rotation O specifying the relative orientation of the vortex planes has vanished.

References

- [1] G. 't Hooft, Phys. Rev. **D 14** (1976) 3432;
C. G. Callan, R. Dashen and D. J. Gross, Phys. Rev. **D 17** (1978) 2717.

- [2] T. DeGrand, A. Hasenfratz and T. Kovács, *Prog. Theor. Phys. Suppl.* **131** (1998) 573.
- [3] Y. Nambu, *Phys. Rev.* **D 10** (1974) 4262;
G. 't Hooft, in: *High Energy Physics*, ed. A. Zichichi (Editorice Compositori, Bologna, 1975);
S. Mandelstam, *Phys. Rep.* **B 23** (1976) 245.
- [4] G. 't Hooft, *Nucl. Phys.* **B138** (1978) 1;
G. Mack, in: *Recent Developments in Gauge Theories*, eds. G. 't Hooft et al (Plenum, New York, 1980);
P. Vinciarelli, *Phys. Lett.* **B78** (1978) 485;
J. M. Cornwall, *Nucl. Phys.* **B157** (1979) 392;
R. P. Feynman, *Nucl. Phys.* **B188** (1981) 479.
- [5] H. B. Nielsen and P. Olesen, *Nucl. Phys.* **B160** (1979) 380;
J. Ambjørn and P. Olesen, *Nucl. Phys.* **B170** [FS1] (1980) 60;
J. Ambjørn and P. Olesen, *Nucl. Phys.* **B170** [FS1] (1980) 265;
J. Ambjørn, B. Felsager and P. Olesen, *Nucl. Phys.* **B175** (1980) 349;
P. Olesen, *Nucl. Phys.* **B200** [FS4] (1982) 381.
- [6] G. 't Hooft, *Nucl. Phys.* **B190** (1981) 455.
- [7] A. Di Giacomo, B. Lucini, L. Montesi and G. Paffuti, hep-lat/9906024; hep-lat/9906025.
- [8] A. S. Kronfeld, G. Schierholz and U.-J. Wiese, *Nucl. Phys.* **B293** (1987) 461;
T. Suzuki and I. Yotsuyanagi, *Phys. Rev.* **D 42** (1990) 4257;
S. Hioki, S. Kitahara, S. Kiura, Y. Matsubara, O. Miyamura, S. Ohno and T. Suzuki, *Phys. Lett.* **B272** (1991) 326.
- [9] G. Bali, Ch. Schlichter and K. Schilling, *Prog. Theor. Phys. Suppl.* **131** (1998) 645, and references therein.
- [10] L. Del Debbio, M. Faber, J. Greensite and Š. Olejník, *Phys. Rev.* **D 55** (1997) 2298.
- [11] K. Langfeld, O. Tennert, M. Engelhardt and H. Reinhardt, *Phys. Lett.* **B452** (1999) 301.

- [12] M. Engelhardt, K. Langfeld, H. Reinhardt and O. Tennert, hep-lat/9904004.
- [13] S. Thurner, M. Feuerstein, H. Markum, W. Sakuler, Phys. Rev. **D 54** (1996) 3457;
H. Suganuma, S. Sasaki, H. Ichie, F. Araki and O. Miyamura, Nucl. Phys. Proc. Suppl. **53** (1997) 528;
S. Sasaki and O. Miyamura, Phys. Rev. **D 59** (1999) 094507.
- [14] H. Reinhardt, Nucl. Phys. **B503** (1997) 505;
C. Ford, U. G. Mitreuter, T. Tok, A. Wipf and J. M. Pawlowski, hep-th/9802191;
O. Jahn and F. Lenz, Phys. Rev. **D 58** (1998) 085006;
M. Quandt, H. Reinhardt and A. Schaefke, Phys. Lett. **B446** (1999) 290.
- [15] R. Bertle, M. Faber, J. Greensite and Š. Olejník, JHEP **9903:019** (1999).
- [16] P. de Forcrand and M. D'Elia, Phys. Rev. Lett. **82** (1999) 4582.
- [17] G. Mack and V. B. Petkova, Ann. Phys. (NY) **123** (1979) 442;
G. Mack and V. B. Petkova, Ann. Phys. (NY) **125** (1980) 117;
G. Mack, Phys. Rev. Lett. **45** (1980) 1378;
G. Mack and E. Pietarinen, Nucl. Phys. **B205** [FS5] (1982) 141;
E. T. Tomboulis, Phys. Rev. **D 23** (1981) 2371;
E. T. Tomboulis, Phys. Lett. **B303** (1993) 103.
- [18] L. Del Debbio, M. Faber, J. Greensite and Š. Olejník, talk presented at the NATO Advanced Research Workshop on Theoretical Physics: New Developments in Quantum Field Theory, Zakopane, Poland, 14-20 June 1997, hep-lat/9708023.
- [19] T. G. Kovács and E. T. Tomboulis, hep-lat/9905029.
- [20] K. Langfeld, H. Reinhardt and O. Tennert, Phys. Lett. **B419** (1998) 317.
- [21] L. Del Debbio, M. Faber, J. Giedt, J. Greensite and Š. Olejník, Phys. Rev. **D 58** (1998) 094501.

- [22] M. Engelhardt, K. Langfeld, H. Reinhardt and O. Tennert, Phys. Lett. **B431** (1998) 141.
- [23] M. Faber, J. Greensite and Š. Olejník, Phys. Rev. **D 57** (1998) 2603.
- [24] M. Faber, J. Greensite and Š. Olejník, Acta Phys. Slov. **49** (1999) 177.
- [25] A. Montero, hep-lat/9906010.
- [26] P. E. Haagensen and K. Johnson, hep-th/9702204.
- [27] R. J. Rivers, *Path integral methods in quantum field theory* (CUP, Cambridge, 1990).
- [28] K. Langfeld, H. Reinhardt and M. Quandt, hep-th/9610213.
- [29] J. M. Cornwall, Phys. Rev. D 58 (1998) 105028.
- [30] J. M. Cornwall, Phys. Rev. D 59 (1999) 125015.
- [31] A. M. Polyakov, Nucl. Phys. **B268** (1986) 406.
- [32] H. Kleinert, Phys. Lett. **B174** (1986) 335.
- [33] A. Hart and M. Teper, Phys. Lett. **B371** (1996) 261.
- [34] R. C. Brower, K. N. Orginos and C.-I. Tan, Phys. Rev. **D 55** (1997) 6313.
- [35] P. Orland, Nucl. Phys. **B428** (1994) 221.
- [36] M. Sato and S. Yahikozawa, Nucl. Phys. **B436** (1995) 100.
- [37] H. Kleinert, *Path integrals in quantum mechanics, statistics, and polymer physics* (World Scientific, Singapore, 1995).